Control of Autonomous Vehicle Platoons

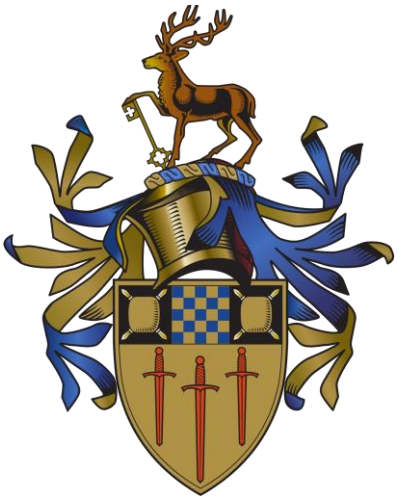

Muazu Imran Wanka
BEng Mechanical Engineering (Hons)

Department of Mechanical Engineering Sciences
Faculty of Engineering and Physical Sciences
University of Surrey

Project Report
May 2019

Project Supervisor: Dr. Umberto Montanaro

Statement of Originality

"I confirm that the submitted work is my own work and that I have clearly identified and fully acknowledged all material that is entitled to be attributed to others (whether published or unpublished) using the referencing system set out in the programme handbook. I agree that the University may submit my work to means of checking this, such as the plagiarism detection service Turnitin® UK. I confirm that I understand that assessed work that has been shown to have been plagiarised will be penalised."

Imran Muazu Wanka

Abstract

Vehicle platooning is presented as a cooperative driving scenario with the potential to significantly enhance and mitigate the drawbacks of road transportation, such as enhancing traffic stability, reducing fuel vehicle fuel consumption, and amplifying highway safety. Under the scope of this documentation, the theoretical concepts of vehicle platooning were investigated as a form of a comprehensive literature review. The final objective of this document is to highlight the necessity of a robust control algorithm to facilitate platooning control aims with respect to network imperfections. To achieve this two separate control algorithms are considered and implemented on a non-linear vehicle model. It is noted that the control strategies were implemented directly on the non-linear model hence negating the mid-level controller. The first controller is time regulating controller based around a proportional-derivative control strategy; this control strategy has a fixed gain, and its practical implementation is on a platoon with a fixed topology. The topology is based upon the information exchange between preceding platoon vehicles and information exchange between the leader and other vehicles within the platoon. The second control strategy is established on a fully adaptive control strategy where the platoon network topology and distributed controllers adapt depending on the relative motion between platoon vehicles, hence enabling the platoon fleet to self-organize based on the creation and maintenance of the control gains. This approach is also fitted with a σ-modification strategy which is used to prevent unbounded drift of adaptive controller gains. Two separate longitudinal vehicle models are investigated, the first is a non-linear vehicle model which is then linearized to form the second linear vehicle model. It is noted that linearization becomes an issue as the mid-level controller is omitted as the control is exerted directly on the non-linear model. Numerical results show the effectiveness of both control strategies to facilitate vehicle platooning objectives with minimal error for a heterogeneous platoon with linear vehicle dynamics. However, the proportional-derivative control is noted as not being able to provide platooning requirements for vehicles with non-linear dynamics effectively. Results highlight the capability of the fully adaptive control approach to make a vehicle platoon self-organizing while limiting the communication links required to maintain cooperative motion between platoon members.

Acknowledgements

I would like to sincere thank everyone who helped me throughout the duration of this project. Most especially my project supervisor Dr. Umberto Montanaro for all the help, support, guidance and time you provided me to successfully accomplish the project aims, despite it being extremely demanding on the technical side for me personally. I am enormously grateful for all of your efforts and this experience was certainly a career defining moment for me. And finally, a massive appreciation to the University, the entire Mechanical Engineering Sciences department specifically for all the support throughout my degree and always giving me help and advice upon my request.

Table of Contents

List of Figures

List of Appendices

List of Tables

Table of Abbreviations

Definition	Abbreviation
Time-gap regulation	TRC
Fully-adaptive	FA
Economic Co-operation and Development	ECD
European union	EU
Formation geometry	FG
Distributed controller	DC
Node dynamics	ND
Autonomous vehicles	AV
Connected autonomous vehicles	CAV
Safe Road Trains for the Environment	SAFTRE
Information flow topology	IFT
Constant distance	CD
Constant headway	CH
Constant time headway	CTH
Non-linear dynamics	NLD
Single-Input-Single-Output	SISO
Model predictive control	MPC
Bi-directional	BD
Linear matrix inequality	LMI
Intelligent transport systems	ITS
Vehicle to everything	V2X
Vehicle to infrastructure	V2I
Vehicle to vehicle	V2V
Predecessor following topology	TPF
Two predecessor following topology	TPLF
Connected adaptive cruise control	CACC
Adaptive cruise control	ACC
Linear time invariant	LTI
Advanced driver assisted systems	ADAS
California Partners for Advanced	PATH
Cloud Assisted Real-time Methods for Autonomy	CARMA
Road side units	RSU
Mobile Edge Computing	MEC
5^{th} generation cellular networks	5G

Table of Notations

Notation	Term	SI unit
N	Number of vehicles in the platoon	-
x_0	Position of the leading vehicle	m
v_0	Velocity of the lead vehicle	ms^{-1}
i_{th}	Preceding vehicle in platoon	-
j_{th}	Ego vehicle in the platoon	-
x_i	Position of generic i_{th} vehicle	m
v_i	Velocity of generic i_{th} vehicle	ms^{-1}
a_i	Acceleration of generic i_{th} vehicle	g
m_i	Mass of a generic i_{th} vehicle	kg
$C_{A,i}$	Lumped coefficient of aerodynamics	-
f	Coefficient of rolling resistance	-
l	Vehicle length	m
A	Vehicle frontal area	m^2
g	Acceleration due to gravity	ms^2
τ_i	Inertial delay in vehicle driveline dynamics	s
T_i	Vehicle driving and braking torque	Nm
$T_{des,i}$	Vehicle driving and braking torque	Nm
$r_{w,i}$	Vehicle wheel radius	m
$\eta_{T,i}$	Mechanical efficiency of the driveline	-
$d_{i,j}$	Gap reduction error between the ego and preceding vehicle	m
t_g	Specified time gap for PD controller	s
x_j	Position of generic j_{th} vehicle	m
v_j	Velocity of generic j_{th} vehicle	ms^{-1}
a_j	Acceleration of generic j_{th} vehicle	g
c_j	Communication delay of generic j_{th} vehicle	s
c_i	Communication delay of generic i_{th} vehicle	s
x_r	Actual distance between preceding vehicles	m
k_1	Controller gain used to form the core of the PD controller	-
k_2	Controller gain used to form the core of the PD controller	-
k_3	Controller gain used to form the core of the PD controller	-
k_4	Controller gain used to form the core of the PD controller	-
h_p	Time gap variables relating to the following vehicles	m
h_l	Time gap variables relating to the lead vehicle	m
k_P	Term used to limit the distance error between preceding vehicles	-
k_l	Term used to limit the distance error between the lead vehicle and other followers	-
p_p	The car following policy of the platoon with respect to following vehicles	-
p_l	The car following policy of the platoon with respect to lead vehicle	-
$\widetilde{a_{ij}}$	Dynamic entry of the adjacency matrix	-
K_{ij}^T	Total adaptive gain entry of FA controller	-
K_{ij}^x	Position adaptive gains for FA controller	-
K_{ij}^v	Velocity adaptive gains for FA controller	--
K_{ij}^a	Acceleration adaptive gains for FA controller	-
e_{ij}^T	Total error mechanism for FA controller	-
e_{ij}^x	Position error mechanism for FA controller	m
e_{ij}^v	Velocity error mechanism for FA controller	ms^{-1}
e_{ij}^a	Acceleration error mechanism for FA controller	g
$\dot{K}_{ij}$	Adaptive mechanism for control gains	-
α	Adaptive mechanism for control gains	-
ρ	Scalar function	-
o	State entry of the potential field	-
B_{ij}	Height of potential barrier	-
U_{ij}	Potential function between two places of stable equilibria	-

F	Forcing error term in potential field	-
λ_{ij}	Damping term potential field	-
SS	String stability criterion	-
M_{ij}	Constant > 0	-
ξ	$\epsilon \{x, v, a\}$	-
Q_{ij}	$Q \epsilon R^{N*N}$	-
ρ_{ij}	$diag(\rho_{ij}^{x}\ \rho_{ij}^{v}\ \rho_{ij}^{a})$	-
$\Upsilon(K_{ij})$	$diag\left(\sigma_{i,j}^{(x)}(K_{i,j}^{(x)})\ \sigma_{i,j}^{(v)}(K_{i,j}^{(v)})\ \sigma_{i,j}^{(a)}(K_{i,j}^{(a)})\right)$	-
$\Pi(e_{ij})$	$[\Upsilon(\boldsymbol{e}_{ij})^{x}, \Upsilon(\boldsymbol{e}_{ij})^{v}, \Upsilon(\boldsymbol{e}_{ij})^{a}]$	-
q	Constant such that $0 < q < 2$	-

1. Introduction

1.1 Cooperative project incentive

An expansion of the world's global economy is projected as the population grows, it is projected that this would lead that this would lead to an increase in the demand for transportation over the coming decades. A prediction was made by the International Transport Forum which predicts that overall freight transportation, measured in tonne-kilometres in organisation for Economic Co-operation and Development (OCECD) countries will increase by 40 to 125% by 2050 compared to the levels in the last decade (Tang, 2014). A significant increase of up to 400% is predicted for developing countries. Road freight transportation accounted for up to 1.7 billion tkm in the European Union and about 3.3 billion tkm in the United States which amounted for 45% and 42% of total freight transport in those regions respectively (Graham et al., 2008).

Transportation is of utmost importance to society, and its demand and effectiveness are strongly related to economic development. Transportation and communication technology from the 20th century form the majority of the current system of trade in most parts of the world. Technological advancements made over the last decade have led to more and more interconnected global markets and have mitigated the costs of transporting, goods, services, and technology around the world (Neophytou, 2016). Road transportation is essential as it accounts for about 60% of all freight transportation which includes all forms of rail and road transport systems (Gamazo, 2013).

Despite the apparent importance of road transport, it faces extreme difficulties such as the need to reduce greenhouse gas emissions and the ever ending rise of fuel prices across the world. Road safety is a significant issue with road transport, according to (NHTSA, 2008) 92% of all road accidents are caused by human recognition error such as inadequate road surveillance and driver distraction and human decision errors such as over speeding. The implementation of intelligent transport systems (ITS) into existing transport systems has enabled the development of a multitude of cooperative driving scenarios to amplify the safety and efficiency of transport networks. Under the scope of this paper, one such approach of cooperative, known as vehicle platooning is investigated.

1.1.1 Environmental incentive for cooperative driving

Energy consumption and emissions have presented enormous challenges due to the increase in demand for road transportation. Under the Kyoto protocol, many industrial countries agreed to reduce greenhouse emissions (Alam et al., 2015). The European Union has also set more ambitious targets to further reduce emissions by 80% to 90% by 2050 considering two decades ago (Alam et al., 2015). This would require a reduction of 60% from the transport sector alone. The transport sector accounted for 33% of the total greenhouse emissions and 24% of the energy usage in the European Union in 2010. At the same moment in time, road transport contributed to 900 million tonnes of CO_2 emissions which is an equivalent of 72% of total greenhouse emissions within all the modes of transportation in the EU (Tang, 2014). A staggering fact is that road transport is the only primary sector of transport which greenhouse emissions are still rising in the European Union (Graham et al., 2008).

1.1.2 Economic incentive for cooperative driving

According to (Alam et al., 2015) fuel prices are going to rise by about 60% in the EU by 2060. As previously stated in this document road transportation is a cornerstone of human economy and society, the rising oil prices would have an adverse effect on society. This reason has led vehicle manufacturers to develop more efficient methods significantly to promote fuel economy. Such methods include the development of more efficient combustions engines and drivetrains, more focus on enhancing aerodynamics, weight reduction, and the development of fuel-efficient tyres. More principles that are fundamental include the implementation of alternative Fossil fuels and the significant development of hybrid and electric vehicles. According to (Graham et al., 2008) a combination of these technological advancements has the potential by 30% in the present day while considering the technologies available at this moment in time.

1.2 Project scope

The objective of vehicle platooning is to ensure all vehicles move at a consistent speed while maintaining a desired spacing policy between the adjacent vehicles in the platoon.

As such, the project aims to showcase the limitations of a vehicle platoon control algorithm with a fixed gain and fixed topology. Therefore the experimental validation of a control algorithm for vehicle platooning that can guarantee platoon formation and control objectives concerning network imperfections will be done to prove the limitations mentioned above.

1.3 Project outline

This document is structured as follows: firstly, key findings and background information obtained from literature will be deliberated and elaborated upon along with the theoretical concepts associated with vehicle platooning. This includes but not limited to the benefits and objectives of vehicle platooning.

In the following chapter, vehicle platoon modelling approaches are investigated. This involves mainly investigation of separate control techniques and the models associated with them. This includes a PD control algorithm and an FA strategy.

In addition, the following chapter explores the experimental procedure used to find numerical results.

Numerical validation and discussion of results are performed afterward, and this involves evaluating numerical findings against distinct testing scenarios. Finally concluding remarks will be made an investigation into any future work improvements.

2. Literature Review

2.1 Vehicle platooning

This chapter is dedicated to establishing the core principles of vehicle platooning and its benefits. Consequently, briefly discussing its main concepts and control specification as obtained from literature. According to (Xu et al., 2014), a vehicle platoon exists as a collection of two or more successive automated vehicles otherwise known as a string of vehicles, moving at a similar speed on the same lane and separated by small distances. The inter-vehicular distance separating the vehicles is defined by a specific spacing strategy or policy. The velocity of the vehicle string is decided by the lead which is either autonomous or human-driven.

The earliest recognised research into vehicle platoon system stemmed from the PATH program during the 1980s in California where many avenues were considered including control structure and architecture, technologies, actuation and longitudinal laws (Shladover et al., 1991). Since its inception, further research avenues of platoon control have been investigated such as the facilitation of powertrain dynamics, selection of spacing criteria, and impact of homogeneity and heterogeneity (Li et al., 2016).

2.2 Cooperative driving principle

Connected autonomous vehicles (CAVs) have been presented as a possible solution to transport such as road safety, traffic congestion, pollutant emissions, and inefficient fuel consumption. Communication systems are used in CAVs to enhance the performance of autonomous vehicles (AV) hence, facilitating cooperative driving and alleviating transport issues. It is noted that this mainly achieved through cooperative manoeuvring and sensing. Cooperative sensing is the process of sharing and fusing information gathered from vehicle sensors and road infrastructure to enable a further understanding of the environment surrounding it. Cooperative manoeuvring refers to the ability of connected vehicles to drive in an organised and coordinated manner in such a way that it is safer for the surroundings and environment.

2.3 Benefits of vehicle platooning

Vehicle platooning possesses several benefits such as 1) enhancing traffic flow, 2) mitigating fuel consumption and reducing pollutants, and 3) improving road safety. These benefits are discussed in detail in the latter parts of this document. It is also considered that vehicle platooning enhances ride comfort and as drivers can focus on other activities during the journey. Vehicle platooning also mitigates the likelihood of jerk during the journey (Ioannou, 1997).

The development of strategy and plans to implement fully functional road trains to facilitate vehicle platooning was carried out by Safe Road Trains for the Environment (SARTRE) research project funded by the European Commission under the seventh framework programme (Arturo et al., 2013). Although vehicle platooning consists of a variety of benefits there exists some challenges in its implementation such as challenges in legislation, public acceptance, and inadequacy of infrastructure to facilitate its successful implementation.

2.3.1 Reduction of fuel consumption and pollutant emissions

The researchers of the SARTRE project carried out fuel consumption simulations to ascertain the fuel reduction potential of vehicle platooning from an aerodynamic perspective. To establish the clear benefits of vehicle platooning, the basic principles of aerodynamics of a moving car in a platoon must be established. When a vehicle is moving on the road, it must overcome rolling resistance and also air resistance.

When a vehicle starts moving it must initially overcome static friction and rolling friction due to the tire contact with the road. According to (Surcel and Shetty, 2015) aerodynamic drag inputs a greater force on the vehicle from between 70 km/hr and 80 km/hr which necessitates a greater power output from the engine which results in more fuel consumption. Figure 1 highlights that 110 km/hr which is the average highway speed, aerodynamic drag approximately equates to 70% of vehicular forces. As stated by (Surcel and Shetty, 2015), 90% of aerodynamic drag is a result of pressure difference in the front and rear end of the vehicle during the ride.

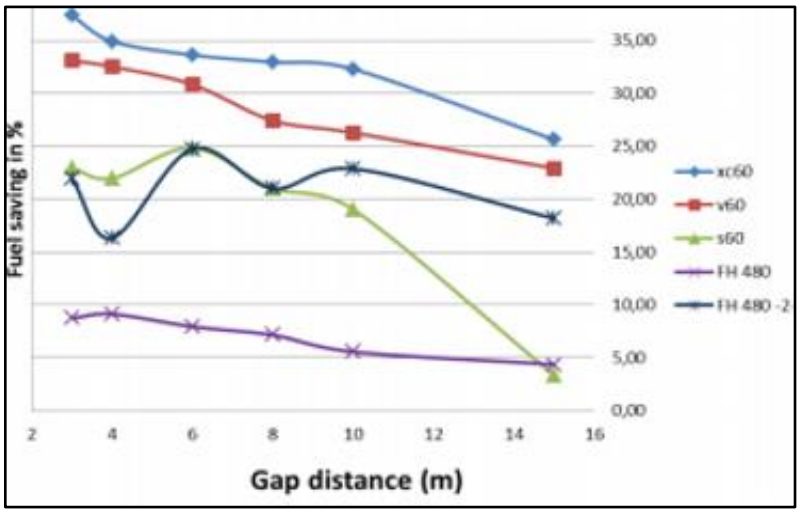

Figure 1: Drag fuel consumption reduction for fuel saving vs gap (Arturo et al., 2013)

During platooning the trailing vehicle will benefit from lower pressure generated by the vehicle in front, thereby leading to reduced aerodynamic resistance as highlighted in Figure 2. This phenomenon becomes bespoke as the gap between the vehicles reduces. The leading vehicle also benefits from the air flow alteration behind it which leads to the reduction of frontal pressure behind it.

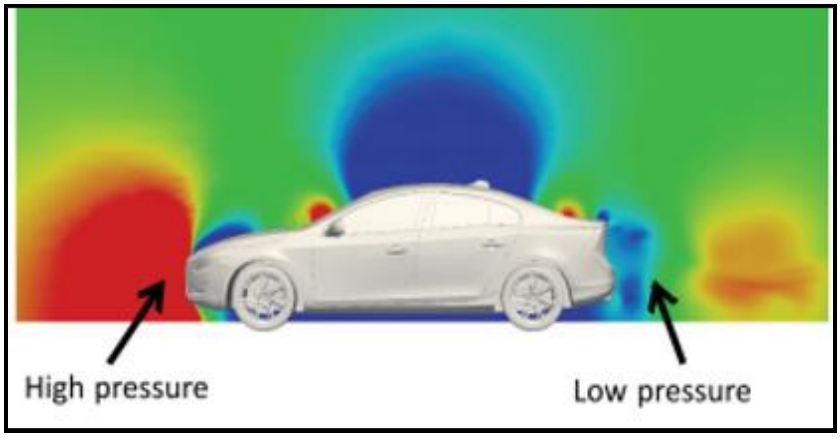

Figure 2: Aerodynamic profile of passenger car (Arturo et al., 2013)

The tests performed during the SARFRE project was made up of a heterogeneous platoon comprising of a lead vehicle truck, and three followers. Figure 3 highlights the fact that as the gap reduces the fuel-

saving increases for the separate cars in the platoon with fuel savings of 7% to 15% at 8 m. Around a range of 8 m to 15 m the behaviour of fuel consumption was steady, as only a slight alteration appeared at 17 m which can be attributed to weather conditions. An increase in fuel consumption appeared at distances of 5 m to 7 m, a further in-depth analysis was carried out to ascertain if this attributed to the effects of aerodynamics in the system. It was also determined that weather did not influence the increase in fuel consumption. (Arturo et al., 2013).

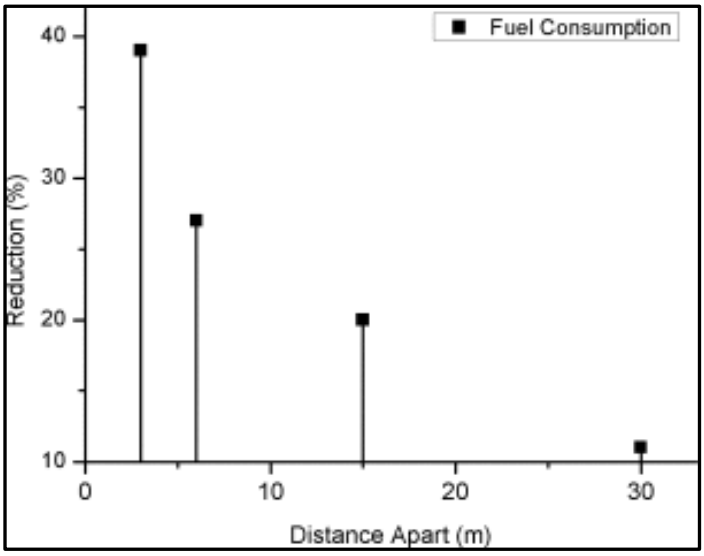

Figure 3: Distance to fuel consumption reduction (Wu et al., 2015)

2.3.2 Improving Traffic Stability and Safety

According to (Kianfar et al., 2012) traffic congestion can be alleviated through the implementation of communication and information technologies by enabling cooperation among vehicles to utilise maximum road capacity. Restricted human perception of traffic conditions and natural constraint on reactional speeds has limited the lower levels of attainable safe inter-vehicular distances. Shock-waves (traffic flow instabilities) could result as a result of erroneous human driving deficiencies. Under dense traffic conditions, a single driver making an error as result of a disturbance such as an emergency stop by the predecessor can trigger a chain of event which could affect the following vehicles and possibly amplify such a disturbance and bring about the complete stop of traffic from miles away, thereby causing a traffic jam for no apparent reason.

This is the reason why string stability is an essential requirement for a vehicle platoon (Sinan et al., 2014). As stated by (Sinan et al., 2014) wireless communication which acts as a means of information exchange between vehicles facilitates a means of overcoming human driving limitations. The effect of different topologies on traffic performance will be discussed in the latter parts of this document.

A study conducted by (Erfan et al., 2016) highlighted that AVs have a positive effect on highways during peak congestion durations. A case in point is the average density of the Autobahn improved by 8.48% during peak congestion hours under an AV scenario. This study on microscopic traffic highlights the potential of AVs to alleviate traffic congestion. As stated in (Erfan et al., 2016) the presence of vehicles in a platoon, drivers tend to maintain a short time head-way. This further substantiates the potential of autonomous platoons on traffic stability.

2.4 Four component framework of a vehicle platoon

In a networked control scenario, a platoon is made up of a series of one dimensional dynamical systems that are connected and automated. (Shengbo et al., 2017). For control objectives to be met, a node (single vehicle in a platoon) only obtains and uses information from other neighbouring nodes to achieve global coordination within the platoon.

As highlighted in Figure 4, a platoon of vehicles is considered moving in a flat road with a generic number of $N + 1$ vehicles, with a leading vehicle referred to as the leader. Thus, the framework of the platoon is divided into four sub-components which are outlined as follows (Zheng et al., 2016).

1. Node dynamics (ND), showcases the longitudinal reaction of individual platoon vehicles
2. Information flow topology (IFT), outlines the mode of information exchange between nodes
3. Formation geometry (FD), outlines the positioning policy amongst the vehicles
4. Distributed controller (DC); it uses information from the (IFT) to implement feedback control

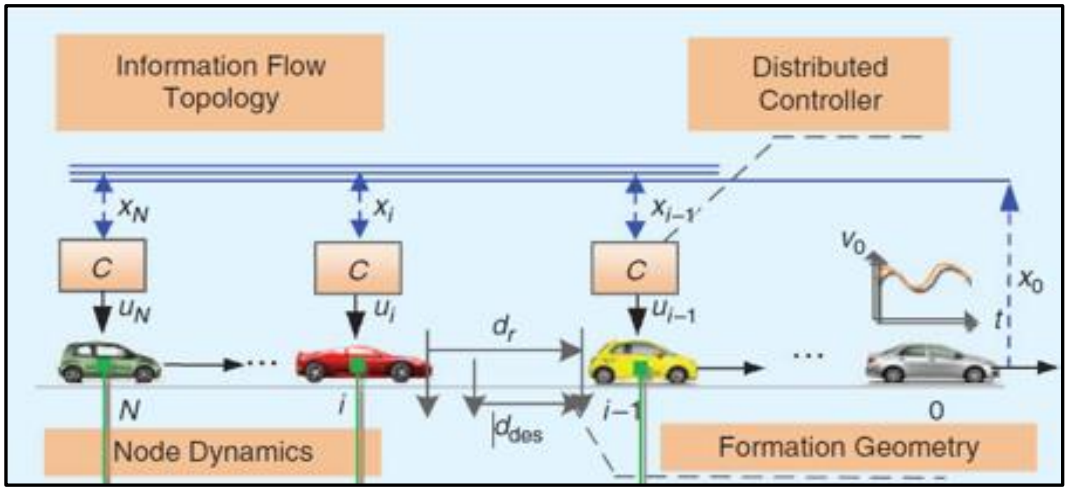

Figure 4: Four component framework of vehicle platoon (Shengo et al., 2017)

2.4.1 Node dynamics

As highlighted by (Ferrara and Vecchio, 2009) most ventures into platoon control make emphasis on longitudinal dynamical behaviours of ND as merely any studies at all integrated longitudinal and lateral control action. The longitudinal dynamics of the vehicle are inherently non-linear due to salient non-linarites in the powertrain such as aerodynamic drag, braking system, engine, and vehicle driveline (Barooah, Mehta and Hespanha, 2009). As outlined by (Xu et al., 2015) studies have directly employed direct nonlinear models for platoon analysis and design.

Adjusting parameters can guarantee string and asymptotic stability. However, performance limitations are rather more complex due to communication topologies and spacing policies for non-linear models. For ease complexity models which are linear are usually used to express controllable complications (Lin, Fardad and Jovanovic, 2013). Frequently used models comprise of:

1) Single integrator model
2) Second-order model
3) Third-order model
4) Single-input-single-output (SISO) model.

A full categorization of relevant literature highlighting these models can be found at (Shengbo et al., 2017). The simplest case is the single integrator model where the control input is characterized as vehicle speed, and the location in the platoon is a select state (Zheng et al., 2018). Due to its inadequacy to accurately depict vehicular dynamics, string stability cannot be attained by the single integrator model.

An acceleration control input is used by both the double integrator model and linear second order model, which forms a foundation for several bases of essential results derived from theory. However, the hypothesis of directly implementing the acceleration as control input is unable to include necessary features of vehicle dynamics such as the inertial interruption in the powertrain will introduce instabilities under realistic driving scenarios (Wang et al., 2014).

One further solution presented is the third order model presented to optimise further the control solution which uses the vehicle engine torque and braking torque as the control input. The pioneering work started by Seiler, Pant, and Hedrick led to the usage of the frequency domain to analyse string stability using a SISO model (Ferrara and Vecchio, 2006) and (Zheng et al., 2018). A platoon is referred to as homogenous when all the followers share identical vehicle dynamics while a platoon is considered heterogeneous when the followers have separate vehicle dynamics (Shaw, 2016). It is noted that the heterogeneous platoon more accurately represents platoon operation under realistic conditions (Zheng, 2016).

2.4.2 Information flow topology

An essential relationship exists between the IFT and the way the vehicles in a platoon obtain information from separately. The IFT uses info from the local controller to describe each node thereby having a profound effect on the overall behaviour of the platoon such as string stability and stability margin (Darbha and Pagilla, 2010) both of which would be discussed in the latter parts of this document some of which are outlined in Figure 5. Early vehicle models vehicle platoons pre-emptively relied upon radars and sensors to close surroundings, this led to the vehicle only capable of acquiring info from the vehicle in front at the rear (Li et al., 2015). This meant that most vehicle IFTs were characterized as either bidirectional (BD) or predecessor-following (PF) types both of which would be investigated under the scope of this documentation. The emergence of advanced V2X communications has resulted in alternative IFTs such as predecessor-following (TPF), two predecessor-leader following (TPLF) type, and the undirected type, a full categorization of theses IFTs is outlined in (Shengbo et al., 2017).

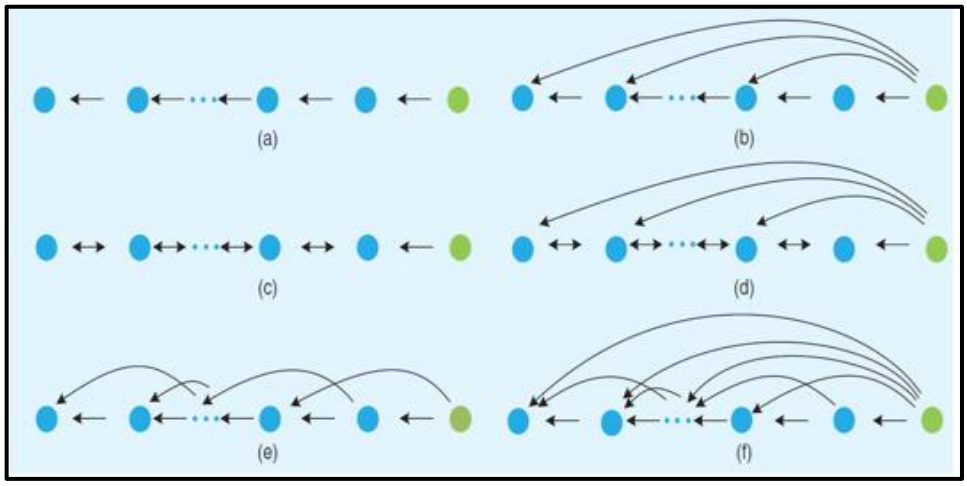

Figure 5: Various platooning topologies (Shengbo et al., 2017)

2.4.3 Formation geometry

The objective of the control of platoon vehicles is to maintain the velocity of the leader at the same time preserving a specific formation directed by the space of the predecessor following vehicles (Zheng and Li 2016). Three central policies exist which govern the FG of a vehicle platoon which are; CD, CTH, and NLD. (Lygeros, Godbole and Sastry, 1998).

2.4.3.1 Constant policy

During the CD policy, the required space between consecutive neighbouring vehicles is kept constant irrespective of the speed of the vehicles which leads to achieving high amounts of traffic volume. This, however, will need more attention needed when defining control parameters and establishing string stability through communication connections; alternatively, a specific stability margin.

2.4.3.2 Constant headway policy

The CTH policy involves varying the vehicle's velocity with the desired inter-vehicular spacing policy. This works better with driver behaviour but is limited in achieving high traffic capacities. To achieve string stability, there exist minimum time headway requirements.

2.4.3.3 Nonlinear policy

The nonlinear policy enables the desired inter-vehicular distance to be a function of the vehicles nonlinear speed which could be used to combat traffic flow instability hence promoting traffic capacity compared to CTH and CD as highlighted by (Zheng et al., 2016).

2.4.4 Distributed controller

The distributed controller is used to implement feedback control be it structured or unstructured using neighbouring information to achieve global coordination (Shengbo et al., 2017). An unstructured DC enables communication between all pairs of vehicles. The IFTs determine the structural property which induces fundamental limitation in platoon performances and difficulty in controller design (Oncu et al., 2014). Stated in (Xiao and Cao, 2011) most DCs are linear to enable easy theoretical analysis and enhanced hardware implementation. DC design is frequently on an individual basis because the structure of an IFT depends on the internal stability of a linear controller (Guo and Yue 2012). As highlighted in (Shengbo et al., 2017) linear control design methods have two significant drawbacks 1) a difficulty exists when trying to handle string stability, 2) they make dealing with non-linarites and constraints difficult. Alternative control strategies were presented in platoons to facilitate better performance. A case in point is (Xiao and Gao, 2016) proposed a sliding mode controller which could guarantee homogenous and heterogeneous string stability. (Roozbeh et al., 2015) implemented an MPC strategy to achieve string stability. (Zheng et al., 2017) to address a control issue with vehicle platoon that has an unknown desired set point in priori introduced an MPC model.

2.5 Closed-loop stability criteria for platoon

This section investigates the control specifications that are fundamental for facilitating platoon control benefits. These properties given within the scope of this project are from a high level viewpoint as such the mathematical foundation of these principles would not be included in this document. There are four key performance metrics the field of platoon control which is internal stability, stability margin, string stability, and coherence behaviour, the last of which would not be discussed in this documentation. The first is used metrics usually define the stability characteristic of the vehicle platoon while the latter of the two focuses on the sturdiness of the vehicle platoon under the influence of external disturbances (Shengbo et al., 2017). Furthermore to these metrics, other factors such as convergence and safety are

paramount in platoon control design a platoon structure though would not be discussed in detail in this document.

2.5.1 String stability

According to (Xiao and Gao, 2011) "String stability indicates the uniform boundedness of all states of the interconnected system for all of the time if the initial states of the interconnected system are bounded." String stability ensures that any slight error in the velocity or position in the leading vehicle will not affect the same states in the following vehicles. String instability may cause collisions and facilitate poor ride quality (Zhou and Peng, 2005). FG and IFN have a strong influence on achieving string stability. According to (Seiler et al., 2004) string stability is strictly not guaranteed for linear controller further down the PF topology and CD policy. Also outlined by (Wu et al., 2016) string stability is severely limited for a homogenous platoon with BD topology using linear equivalent controllers.

This work was further extended string stability cannot be altered using both forward communication range and small-time headway when considering a platoon of heterogeneous ND (Middleton et al., 2010). Both (Xiao and Gao, 2011) and (Naus et al., 2010) have proposed a solution to enhance string stability using relaxing forming rigidity which mainly involves introducing sufficient time headway for spacing policy. Another solution was the use of more complex IFTs (Shaw and Hedrick, 2007) and also using non-identical controllers for separate vehicles (Barooh et al., 2009). Some recent studies have proposed an advanced controller to enhance string stability. This includes a sliding mode controller proposed by (Xiao and Gao, 2011) and a model predictive control by (Kianfar et al., 2012).

It is important to note that both control algorithms implement a CTH policy and make use of the leader's information (Ploeg et al., 2014). Present day research is concentrated around the probability of encountering external disturbances by both the leader and the following vehicles. String stability is represented in the Laplace domain according to (Naus et al., 2010) according to 2.1.

$$SS(s) = \frac{X_i(s)}{X_{i-1}(s)} \leq 1, \; i \geq 2 \qquad 2.1$$

As stated by (Hobert et al., 2015) platoon control solutions usually take advantage of vehicle-to-vehicle (V2V) or vehicle-to-everything (V2X) communication interfaces to showcase platoon control design topology. Network induced imperfections are introduced such as packet loss and latency are introduced when studying the robustness of the closed-loop system concerning communication introduced to the system (Harfouch et al., 2017). Noted by (Hobert et al., 2015) communication imperfections are considered as switches within platoon topologies as disturbances hence, the platoon control scheme is regarded as stable concerning the abrupt variations in the topology.

As highlighted by (Cao et al., 2017), the expected enhanced performance of the 5G is poised to mitigate significantly network imperfections such as latency which could hugely impact vehicle platooning. This is why studies such as one carried out by (Zheng et al., 2017) have presented ideal network platoon control methods. As previously proven by (Zheng at al., 2017), the variety of control gains used to guarantee closed-loop stability is affected by the topology.

As highlighted by (Cao et al., 2017), the expected enhanced performance of the 5G is poised to mitigate significantly network imperfections such as latency which could hugely impact vehicle platooning. This is why studies such as one carried out by (Zheng et al., 2017) have presented ideal network platoon control methods. As previously proven by (Zheng at al., 2017), the variety of control gains used to guarantee closed-loop stability is affected by the topology.

As stated by (Al Ridhawi et al., 2018), CAVs can also leverage MEC platforms together with an enhanced communication network. These servers will aid in collecting data from vehicles, roadside sensors, and process analysed data hence, distributing these latency sensitive messages to the platoon by leveraging the low latency of 5G networks. These MEC servers will be connected at RSUs to mitigate

round-trip. These messages can be used on board be the vehicles which enhance vehicle platoon performance. The CARMA development is currently investigating the feasibility of implementing 5G communication with MEC servers (Stevens et al., 2017). The use of this technology could lead to new ways of platoon control where the network topology could be adapted in real-time relative to vehicle dynamics. This accommodates the self-organisation of the vehicle in the platoon to attain synchronous motion. A study by (Montanaro et al., 2018) proposed an approach on how the CARMA framework can be used to back vehicle platoons with changing topologies. However, as mentioned in the study there are a few complications such the choice of control gains to achieve compliant movement and the necessity to mitigate the burden on the communication network by decreasing the links between the topologies.

2.5.2 Internal stability

According to (Darbha and Pagilla, 2010) a linear time-invariant platoon is internally stable strictly when the eigenvalues of the closed-loop system are negative under any circumstance. Regardless of the sort of platoon topology adopted, internal stability must strictly be guaranteed. Two distinct approaches were suggested to ensure internal stability namely 1) global approach (Guo and Yue, 2011) and 2) local approach (Zheng et al., 2016). As noted by (Zheng et al., 2016), it is possible to consider the platoon as an organized scheme and designed the regulator in a centralised method to prevent the IFT being significant in the strategy procedure.

A case in point (Guo and Yue, 2011) guaranteed internal stability by obtaining linear matrix inequality (LMI) centred on the over-all vehicle platoon dynamics. A fundamental shortcoming of the methodology is the fact that it introduces computational inefficiencies with an increase in platoon size. Outlined in (Ploeg et al., 2014) this led to a variety of studies decomposing a platoon into a variety of sub-systems and applying the decentralized control method. The PF topology enables a platoon to exist and logically viewed as a mono-directional flow of structures. As such, it is merely necessary to guarantee string stability as shown in (Xiao and Cao, 2007). According to (Stankovic and Stanojevic, 2000) inclusion principle can be leveraged to break down such a platoon into a native sub-system in a situation where an overlying controller was designed.

This procedure is however not appropriate for a BD type topology because the mismatch spread in both ways. Some studies such as (Hao and Mheta, 2011) exercised partial differentiation (PDE) techniques to estimate platoon dynamics of BD topologies. This could enable the escape analysis of advanced dimensional dynamics. The Lyapunov method was implemented by (Liu and Murray, 2004) to prove latitudinal lane keeping stability and longitudinal car following stability. LaSalle's invariance standard can also be implemented in order to showcase asymptotic stability for time-variant platoon schemes in cases where the derivative of the Lyapunov function is negative semi-definite.

2.5.3 Stability margin

Stability margin can be defined as a functioning parameter that characterizes the merging velocity of preliminary mismatch in a platoon (Ploeg et al., 2014). Most discoveries have focused on CD policies for stability margin study, which also defined the performance index to be a parameter of 1) platoon size 2) ND, 3) DC structure, and 4) IFT (Barooah et al., 2011). It was proven by (Barooah et al., 2011) by leveraging ND as a point mass, a small amount of mistuning could be introduced to prove that asymptotic behaviour of stability margin as $O(1/N^2)$ under symmetric bidirectional control. Also, (Zheng and Li, 2016) later furthered this result to third-order dynamics which were linear included inertial vehicle delay in the powertrain. Proven by (Hao and Barooah, 2016), stability margin was capable of bounding away from zero irrespective of the size of the platoon.

3. Vehicle Platoon Modelling and Objective

3.1 Platoon control objective

Consider a series of adjacent vehicles depicted in Figure 6, where v_0 represents the velocity of the leading vehicle and d_{ij} portrays the desired relative distance of two preceding following vehicles *j* and i respectively. Where $i \in N$ and N refers to the number of vehicles in the platoon. Consequently, the control of a vehicle platoon can be considered to be a twofold problem where the aim is to:

1) Enforce the leader velocity v_0 on all following N vehicles in the platoon.
2) Regulate the distance between two preceding vehicles using a pre-defined spacing policy between an i_{th} vehicle and j_{th} vehicle, i.e. the control objective can be defined as follows when the leader of the platoon is travelling in a steady state velocity such that its acceleration $a_0 = 0$. (Zheng et al., 2016).

$$\lim_{t\to\infty} \left|\left|v_i(t) - v_0(t)\right|\right| = 0 \qquad 3.1$$

$$\lim_{t\to\infty} \left|\left|x_j(t) - x_i - d_{i,j}\right|\right| = 0 \qquad 3.2$$

3.2 Longitudinal vehicle dynamics

This section is devoted to exhibiting platoon control objectives, outline model for vehicle longitudinal dynamics and show model of platoon network which would be used to formulate the FA control architecture in the latter parts of this document as obtained from literature.

As discussed in earlier parts of this document a vehicle platoon can be viewed as a collection of vehicles that can otherwise be referred to as nodes. The longitudinal dynamics of every node can be viewed as being inherently non-linear. Thus, consisting of but not limited to the engine, driveline, aerodynamic and frictional forces, and braking system. Under the scope of this documentation, two separate vehicle dynamical models would be considered for the depiction of platoon vehicles. As stated in (Eben Li, Li and Wang, 2013), and (Li et al., 2011) some assumptions are exercised to obtain a model capable of facilitating control as follows:

1. Driving and braking torque are assumed inputs capable of being controlled.
2. Vehicle pitch and yaw moment are neglected to enable simplicity.
3. The vehicle body is assumed symmetric and rigid.
4. The longitudinal slip of the tyre is rendered as insignificant while the powertrain dynamics is lumped into a first order inertial transfer function.

Table 1: Frequently used terms in vehicle platooning within project scope

Symbol	Term	Physical significance
x	Position	Vehicle position within platoon
v	Velocity	Vehicle velocity within platoon
a	Acceleration	Vehicle acceleration within platoon
d	Distance	Distance between consecutive vehicles
i	Preceding vehicle	Preceding vehicle follower
j	Ego vehicle	Ego vehicle follower
e	Error	Error term for any variable
0	Lead vehicle	Lead vehicle

3.2.1 Non-linear vehicle model

As explored in both (Naus et al., 2010) and (Guo and Yue, 2011) longitudinal vehicle dynamics are inherently non-linear and can be expressed as follows:

$$\dot{x}_i(t) = v_i(t) \tag{3.3}$$

$$\frac{\eta_{T,i}}{r_{w,i}} T_i(t) = m_i \dot{v}_i(t) + C_{A,i} v_i^2(t) + m_i g f, \quad i \in N \tag{3.4}$$

$$T_{des,i}(t) = \tau_i \dot{T}_i(t) + T_i(t) \tag{3.5}$$

Outlined in Table 1 below are frequently used terms in vehicle platooning within the scope of this project. The purpose of this table is to ease the readability and enhance the clarity of the body of this document.

3.2.2 Linear vehicle model

An exact feedback linearization technique showcased by (Zhang et al., 1999) and (Ghasemi, Kazemi and Azadi, 2013) can be used to adapt the non-linear model to a linear model hence facilitating simplicity of controller design. Where the feedback linearization law is denoted in 3.6 below. It is noted that the mid-level control action represented in 3.4 is disregarded within the scope of this project. As such, the feedback linearization technique is noted to present an issue as the control law is directly exerted on the non-linear model.

$$T_{i,des}(t) = \frac{1}{\eta_{T,i}} \left(C_{A,i} v_i (2\tau_i a_i + v_i) + m_{i,ve} g f + m_{i,ve} u_i \right) r_{w,i} \tag{3.6}$$

Linearized longitudinal dynamics is derived when the u is the new control input signal upon linearization as such a third order state space model is represented as follows, Where the state of each vehicle i is denoted as in 3.7;

$$S_i(t) = [x_i, v_i, a_i]^T \tag{3.7}$$

$$S_i(t) = \begin{bmatrix} x_i \\ v_i \\ a_i \end{bmatrix}' A_i(t) = \begin{bmatrix} 0 & 1 & 0 \\ 0 & 0 & 1 \\ 0 & 0 & -\frac{1}{\tau_i} \end{bmatrix}' B_i = \begin{bmatrix} 0 \\ 0 \\ \frac{1}{\tau_i} \end{bmatrix} \tag{3.8}$$

3.3 Network model for platoon control

The problem of vehicle platoon control can be depicted as an interface of multi-agent system on a network platform (Zheng et al., 2017) that is controlled in a way to enable the dynamics of the nodes (individual follower dynamics) to converge towards the pinner mode i.e. leader dynamics (Wang and Su, 2014). These networked dynamical systems can be group into three components as follows (DeLellis, di Bernardo and Porfiri, 2011).

1. The dynamical behaviour of each node when disconnected from the network.
2. The various topologies used to describe nodal connections within the network.
3. The control action used to guide each node towards the trajectory of the pinner mode.

The topology of N number of followers in a vehicle platoon can be represented in a finite graph as a pair $G_N = (V_N, E_N)$. Where the set of nodes within the network are $V_N = \{1,2, \dots N\}$ and the edges of the network are stated as $E_N \subseteq V_N \times V_N$. When the i_{th} and j_{th} vehicle in the platoon are elements of the network edges (DeLellis, di Bernardo and Porfiri, 2011). The adjacency matrix of the graph can be defined as $A_N \in R^{N \times N}$ based on E_N.

As such the generic entry of the adjacency matrix, A_N can be defined as $a_{ij} = 1$ when the i_{th} vehicle receives information from the j_{th} vehicle else $a_{ij} = 0$ when there is no exchange of information. It is also noted that it is not possible for any generic node entry within the network to receive information from itself i.e. $a_{ii} = 0$. The graph G_N is used to represent the pinner of the network which is the platoon leader, therefore given as $G_{N+1} = (V_{N+1}, E_{N+1})$. The corresponding adjacency matrix yields $A_{N+1} \in R^{N+1 \times N+1}$ such that $a_{0j} = 0$ where $j = 0,1,2 \dots N$.

4. Control algorithms

4.1 PD time-regulating control architecture

The structure of the PD controller permits the distance gap reduction error $d_{i,j}$ between the ego and preceding vehicle. Where the error is characterized by a specified time gap t_g which is implemented to maximize error reduction capabilities and enhance safety. The relative error between the two vehicles as shown in Figure 8 is given by the expression in 4.1 as follows. A similar control structure was explored in (Milanés et al., 2014).

$$d_{i,J} = x_r - v_i t_g \quad 4.2$$

To guarantee string stability of the platoon (Shengbo et al., 2017), wireless network communications must be facilitated between the vehicles. This is also paramount in guaranteeing the safety of the vehicles and enhancing vehicle response. As shown in Appendix 10 the terms c_j and c_i are used as communication delay terms in the ego and preceding vehicles respectively. The terms x_0 and x_i represent the position of the leader and preceding vehicle in the platoon.

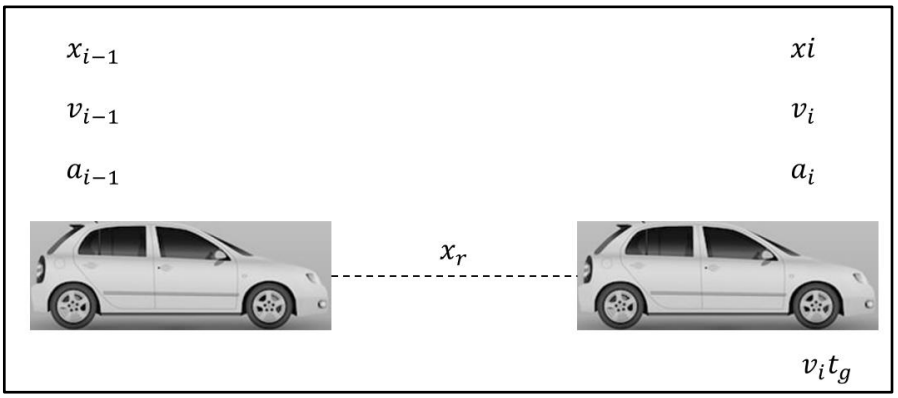

Figure 6: Adjacent platoon vehicles

To achieve the time-gap structure mentioned above, a PD control strategy is leveraged to achieve stability with respect to the leading vehicle and immediate preceding vehicle in the platoon as portrayed in Figure 6. This results in the combination of two time gap error regulation PD controllers both of which are used to achieve the objective mentioned above. A state space representation of this control structure is represented in two parts and outlined as follows:

$$u_i(t) = k_1 x_i + k_2 v_i \quad 4.3$$

$$u_0(t) = k_3 x_0 + k_4 v_0 \quad 4.4$$

The car following policy of the platoon correspond to terms $p_0(t)$ and $p_i(t)$ which are used to govern the time-gap specification mentioned above.

$$p_i(t) = x_i + h_i v_i \quad 4.5$$

$$p_0(t) = x_0 + h_0 v_0 \quad 4.6$$

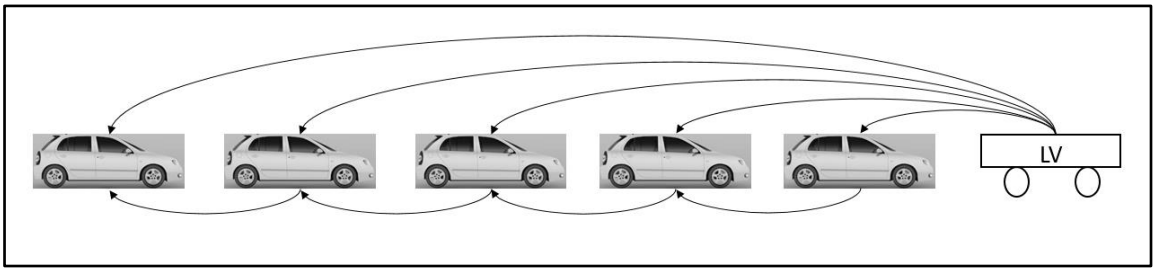

Figure 7: PD control platoon network topology

As shown in Appendix 10 the controller is made up of three main parts. One part is used to maintain a specified velocity v_i of a generic i_{th} within the platoon without considering the speed of the ego and preceding vehicle (Bu et al., 2010), as such the target speed of the preceding v_j is leveraged as a feedforward term for the platoon. This facilitates vehicle velocity response and enhances delay reduction in throttle-brake actuation transition (Milanés et al., 2014).

As noted in (Xiao and Gao, 2011) this sort of control architecture with a fixed gain and fixed topology has certain drawbacks due to lag in the vehicle peripherals such as actuators, sensors, and the powertrain. These are not ideal for string stability and provision of efficient platoon control performance. As stated in earlier parts of this documentation for control simplicity, these drawbacks are lumped to form pure time lags in throttle and engine actuation, engine response, and low-pass filters used in various sensors in the vehicle.

According to (Shladover et al., 2012) when a platoon vehicle receives information only from its predecessor vehicle, specified time-headway would need to be increased to at least half of the value of the lump parasitic delay and lag to guarantee string stability of the platoon. Increasing time headway principally involves increasing inter-vehicular distance, which reduces the benefits of platooning due to a reduction in fuel efficiency and less road usage efficiency.

4.2 Fully adaptive control architecture

The FA control architecture explored within the scope of this document would be evaluated to demonstrate the drawbacks of the PD controller mentioned above. The primary purpose of this is to highlight the ability of an adaptive controller to guarantee platooning objectives stated in 3.1 and 3.2 satisfy the string stability criterion. Under this section the networked model used in the control architecture as well as the functional operability of the control action would be discussed.

The fully adaptive control architecture leverages the theory of adaptive networks to create the control gains and make the arcs of the topology mentioned in the previous chapter adaptive based on the error between platoon member dynamics. Where the state error between two platoon errors is given in 4.7 where $i = 1,2,3 \dots N$ and $j = 0,1,2,3 \dots N$. The coefficients of the adjacency matrix are donated as A_{N+1} of $\mathrm{G_{N+1}}$.

$$e_{ij}^{T} = [e_{ij}^{(x)}\ e_{ij}^{(v)}\ e_{ij}^{(a)}] \tag{4.7}$$

$$e_{ij}^{(x)} = x_i - x_j - d_{ij} \tag{4.8}$$

$$e_{ij}^{(v)} = v_i - v_j \tag{4.9}$$

$$e_{ij}^{(a)} = a_i - a_j \tag{4.10}$$

The control action u_i is given as follows according to the information the j_{th} vehicle sends to the i_{th} vehicle where the i_{th} computes the control action as in 4.11. A similar control structure was used in (Petrillo et al., 2018).

$$u_i = -\sum_{j:j\in N_i} a_{ij}(t)K_{ij}^T(t)e_{ij} \tag{4.11}$$

$$K_{ij}^T(t) = \left[K_{ij}^{(x)}(t)\ K_{ij}^{(v)}(t)\ K_{ij}^{(a)}(t)\right], \quad (j,i) \in E_{N+1} \tag{4.12}$$

From the theory of adaptive networks each entry of the adjacency matrix can be represented as a second order state system evolving in a potential field as in 4.13

$$\ddot{o}_{ij} + \lambda_{i,j}\dot{o}_{ij} + \frac{dU_{Ij}}{do_{ij}}(o) = F\left(\left|\left|e_{Ij}\right|\right|_{Qij}\right) \tag{4.14}$$

$$a_{ij}(t) = o^2(t), \qquad (j,i) \in E_{N+1} \tag{4.15}$$

$$U_{ij}(o) = 16B_{ij}o^2(o-1)^2, \qquad (j,i) \in E_{N+1} \tag{4.16}$$

The dynamic entry of the adjacency matrix can be depicted as a unitary mass $\dot{m}_{i,j}$ system evolving in a potential field subject to linear damping λ and an external force F acting in the opposite direction as shown in Figure 8 Due to the need for limiting the overall network load, the entry of the adjacency matrix a_{ij} between two generic nodes (i,j) within the network will converge to 0 and 1 respectively where 0 and 1 are places of stable equilibria within the network (DeLellis, di Bernardo and Porfiri, 2011). Suppose the error e_{ij} between two nodes within the platoon network topology is negligible then, a_{ij} will converge to 0 and the corresponding arc G_{N+1} of the network topology can be removed. As such the i_{th} vehicle will compute its control action u_i without receiving information from the j_{th} vehicle. Consequently, if the error between two nodes is not negligible then the arc is maintained and the control action of the i_{th} vehicle is kept and calculated according to 4.17 whilst using information from the j_{th} vehicle. Where B_{ij} is represented by the height of the potential field that separates the two regions of stable equilibria i.e. 0 and 1 in Figure 8.

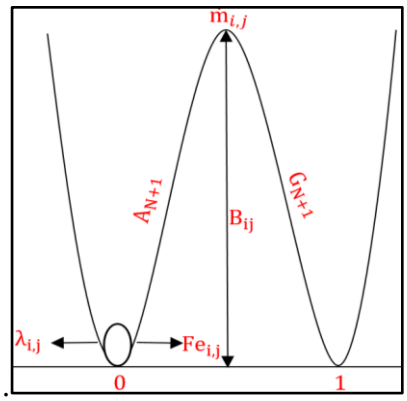

Figure 8: Unitary mass in potential field

The control presented in 4.18 is an inclusion of control approaches presented by (DeLellis, di Bernardo and Porfiri, 2011) and (Zheng et al., 2017) although when platoon control such as in 4.3 and 4.4 the platoon topology becomes fixed such as in Figure 7, network overload cannot be prevented hence, prompting network imperfections such as latency and packet loss. The adaptive mechanism used for control gains is selected according to (4.17). The adaptive mechanism depends on the corresponding error vector as depicted in (4.18).

$$\dot{K}_{ij} = \alpha_{ij}\Pi(e_{ij}) - \rho_{ij}\Upsilon(K_{ij})K_{ij} \tag{4.19}$$

$$\dot{K}_{ij} = \begin{bmatrix} K_{ij}^{(x)} \\ K_{ij}^{(v)} \\ K_{ij}^{(a)} \end{bmatrix} = \begin{bmatrix} \left| \frac{e_{ij}^{(x)2}}{1+e_{ij}^{x}} \right| \\ \left| \frac{e_{ij}^{(v)2}}{1+e_{ij}^{x}} \right| \\ \left| \frac{e_{ij}^{(a)2}}{1+e_{ij}^{x}} \right| \end{bmatrix} \tag{4.20}$$

The adaptive control law allows ensures the derivative of the control gains $\dot{K}_{ij}$ to remain bounded in the presence of a significant mismatch between vehicles. It is also important to note that the magnitude of the control gains remain bounded when subjected to external disturbances and un-modelled dynamics as the adaptive mechanism highlighted in 4.19 contains the σ-modification factor $\sigma_{i,j}^{(\xi)}\left(K_{i,j}^{(\xi)}\right)$ which ensures the control of adaptive gains is outlined in 4.21.

$$\sigma_{i,j}^{(\xi)}\left(K_{i,j}^{(\xi)}\right) = \begin{cases} 0 \\ \left(\frac{K_{i,j}^{(\xi)}}{M_{i,j}^{(\xi)}} - 1\right) \end{cases} \tag{4.21}$$

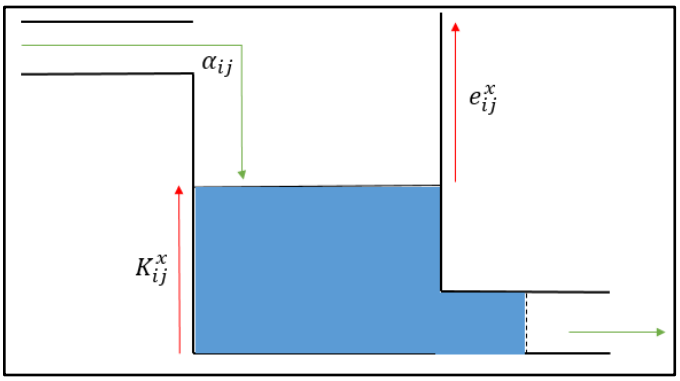

Figure 9: Adaptive gains analogy

This strategy can be depicted using a water tank analogy can be used to depict how the growth of a corresponding adaptive gain can be limited. Consider Figure 9 where the adaptive gain of the position $K_{ij}^{(x)}$ is denoted. The position error e_{ij}^{x} is characterized by the water level in the tank, as such the corresponding control action is activated based on that water level. When the water level exceeds a certain specified level the term used to prevent the unbounded drift of control gain $\gamma\left(e_{i,j}^{(\xi)}\right)$ depicted as the valve on the tank is opened which empties the water and returns it to the pre-specified level. The σ-modification strategy is used to control the water level entering the tank which ensures the error e_{ij}^{x} does not increase beyond the pre-specified level. This depicts how the growth of the adaptive gains are limited thus, enabling their decrease when they exceed beyond a specified threshold.

5. Simulation Setting and Control Design

5.1 Simulation procedure

Control algorithms mentioned in 4.3, 4.4 and 4.11 were experimentally validated via MATLAB and Simulink. For this case study, the controller was tested via Simulink simulations for both linear and non-linear vehicle dynamics respectively. The effectiveness of both controllers to facilitate platooning control objectives suggested in 3.1 and 3.2 were numerically tested for a heterogeneous vehicle platoon consisting of 5 vehicles. The initial states of the vehicles were chosen in such a way that there was no collision initially at $t = 0\ s$.

Furthermore, this was also done to test the ability of the controller to satisfy the string stability criterion in 2.1 for the vehicle platoon. For both control action experiments, the inertial dynamics of the lead vehicle will be represented as linear as in 3.7. The time constant used to depict time constant of the leader in every scenario as in 3.8 was chosen as $0.1\ s$. The initial state of the leader state was chosen as $[100\ 75\ 0]$ respectively where each term is the initial position, velocity, and acceleration of the leader respectively within the platoon.

Consider Figure 10 where the first manoeuvre consists of two separate sub-manoeuvers, the first is depicted as an initial series of trapezoid shapes from $t = 0 \leq t \leq 290\ s$ which represent normal vehicle behaviour under braking. The manoeuver is made up of several constant velocity stages of $75\ km/hr$ and consequent acceleration manoeuvers of $90\ km/hr$. The second manoeuver from $t = 290\ \leq t \leq 360\ s$ represents the vehicle behaviour under emergency braking conditions which is represented by the sinusoid shape which constitutes of an increase of leader speed from $75\ km/hr$ to $90\ km/hr$ in time spurts of $5\ s$ with a period of $15\ s$.

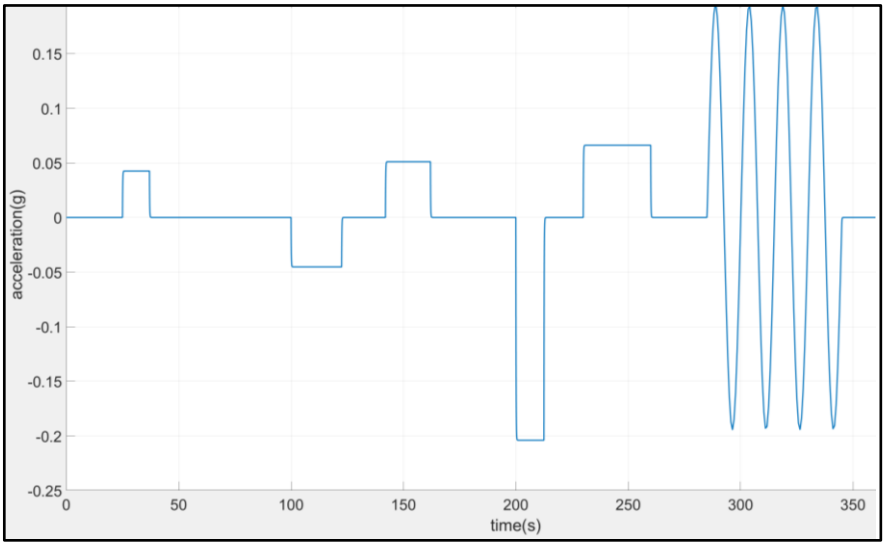

Figure 10: Leader manoeuver for normal and emergency braking reference input

The second manoeuvre can be characterized as a so called "door function" which is made up of two separate step functions. This manoeuvre was craeted to depict constant vehicle velocity from $0 \leq t \leq 148\ s$, then an acceleration manoeuvre at $t = 148\ s$ which is consequently followed by a deacceleration at $t = 152\ s$, the manoeuvre concludes with constant velocity from $152 \leq t \leq 360\ s$.

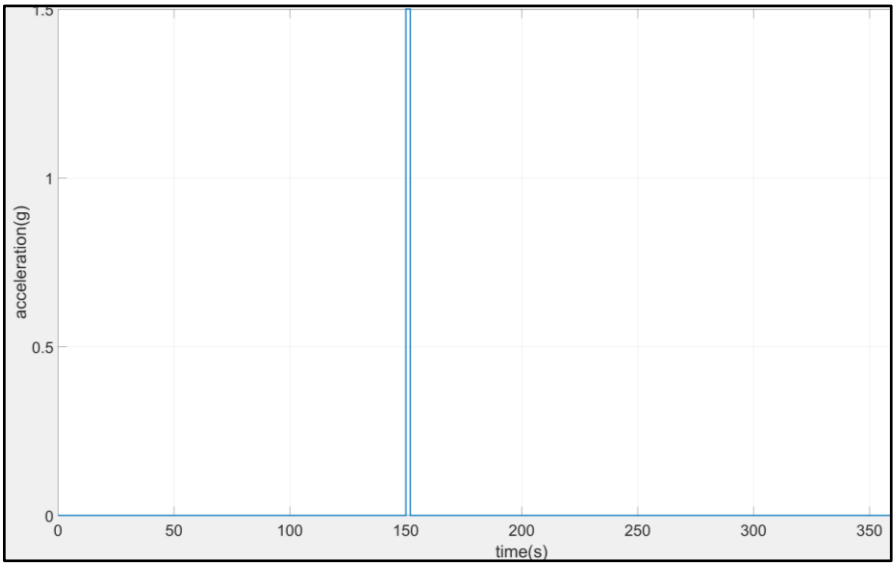

Figure 11: Leader manoeuver for door reference input

5.1.1 Time regulating control strategy

Outlined in Table 2 are the final parameters for the representation of the PD control strategy parameters. Controller gains were selected as a non-trivial trade-up between the convergence of vehicle inter-vehicular distance and obtaining realistic velocity and acceleration values respectively for each vehicle. For this experimental evaluation, two separate vehicle manoeuvres were evaluated as in Figure 10 and Figure 11.

$$E_{rr} = \begin{matrix} 1 & -1 & 0 & 0 & 0 & 0 \\ 0 & 1 & -1 & 0 & 0 & 0 \\ 0 & 0 & 1 & -1 & 0 & 0 \\ 0 & 0 & 0 & 1 & -1 & 0 \\ 0 & 0 & 0 & 0 & 1 & -1 \end{matrix} \quad 5.1$$

Denoted in 5.1 is an error matrix E_{rr} used to depict relative mismatch between vehicles on MATLAB which ensured the production of results included in the preceding chapter of this document. This was obtained based on the topology mentioned in Figure 7 where preceding vehicles obtain information from each other. The ego vehicle is represented by 1 and -1 represents a preceding vehicle

Outlined in Appendix 9 is a model of the PD control structure implemented on Simulink. It represents the influence and dependencies of controller gains on time gap specifications. Shown in Appendix 7 is the representation of a Simulink model used to depict the lead vehicle and 5 platoon followers where the inertial dynamics of the lead vehicle was linear, and the dynamics of the followers was non-linear.

5.1.1.1 Linear vehicle dynamics

A desired time gap of 0.5 s was used as the time gap following policy between both the lead vehicle and preceding vehicles. A communication delay of 0.2 s was included in the test model to depict delay in wireless communication between a generic i_{th} and j_{th} vehicle. This parameter was chosen as a realistic value to depict the delay in 4G communications transmission across platoon vehicles according to (Lari, 2018). To depict the heterogenic nature of the platoon the inertial delay in driveline dynamics τ was varied such that $0.1 \leq \tau \leq 0.8$. It is noted that this was done at no particular order and does not compromise the validity of the results. The MATLAB model used in shown in Appendix 8.

Table 2: Linear vehicle parameters used in simulation

Parameter	Numerical value
K1	12.88408
K2	0.038555
K3	100
K4	0.005
h_p	0.5
h_l	0.5
c_i	0.2
τ_i	$0.1 \leq \tau_i \leq 0.8$

5.1.1.2 Non-linear vehicle dynamics

To depict heterogenic nature of the platoon a range of variables mentioned in 3.6 were altered for separate vehicles. The parameters used in 3.4 and 3.6 are shown in Table 3. The vehicle mass m was chosen as a range of $800\ kg \leq m \leq 1600\ kg$. The length of the vehicle was varied between $4.5 \leq l \leq 5\ m$. The mechanical efficiency of the driveline η_T was chosen over a range of $0.82 - 0.92$. the internal lag of the driveline was chosen as in the linear model mentioned above. The driveline control action T_{des} shown in 3.6 is the output torque of the engine driveline.

Table 3: Non-linear vehicle parameters used in simulation

Parameter	Numerical value
C_A	$0.2 \leq C_A \leq 0.6$
g	9.81
f	0.01
$r_{w,i}$	0.34
$\eta_{T,i}$	$0.82 \leq \eta_{T,i} \leq 0.92$
m	$800 \leq m \leq 1600$
τ_i	$0.2 \leq \tau_i \leq 0.8$
ρ	1.225
l_i	$4.5 \leq l_i \leq 5$
A_i	2.24
$K1$	0.03855
$K2$	9.797
$K3$	893.5
$K4$	0.002
h_p	0.5
h_l	0.5
c_i	0.2

5.1.2 Fully adaptive control strategy

The FA control strategy was evaluated according to 4.11 using MATLAB and Simulink. For reasons of intellectual property the MATLAB code and Simulink diagrams used in the evaluation of the control algorithm are not included in the body of this report for brevity. The evaluation of the control algorithm was done to prove the necessity of having a controller capable of overcoming the shortcomings of the PD control structure as shown in Figure 18. It is explicitly noted that all experimental work carried out within the scope of this project regarding the FA control strategy was done for testing and numerical validation purposes only as such no controller design was actually carried out within the scope of this

project. The evaluation of the controller was done under the same conditions mentioned in the earlier parts of this chapter, although slight alterations were made due to the heterogenic nature of both controllers. These parameters are outlined in Table 4.

Table 4: FA controller evaluation parameters

Parameter	Numerical value
C_A	$0.99 \leq C_A \leq 1.17$
g	9.81
f	0.02
r_w	$0.30 \leq r_w \leq 0.39$
η_T	$0.82 \leq \eta_T \leq 0.92$
m	$1035 \leq m \leq 1819$
τ	$0.51 \leq \tau \leq 0.78$
ρ	1.225
l	5
A	2.24
$B_{0,i}$	5
$B_{i,j}$	$1 \leq B \leq 0.1$
λ	$0.1 \leq \lambda \leq 5$
c_i	0.2

6. Results and Discussion

6.1 Numerical validation

Presented in this section is numerical validation of control algorithms mentioned in the earlier parts of this document. The results presented are only aimed at proving the capability of each controller mentioned in this section to facilitate platoon control objectives mentioned in 3.1 and 3.2. As such all other tests carried out to showcase the effectiveness of control algorithms such as the position, velocity and acceleration profiles of platoon vehicles during various vehicle manoeuvres are considered trivial hence, included in the Appendix of this report. Outlined in Table 5 below is a error index that would be used throughout this chapter. It is important to note that where legend entries are not displayed within the graphical results of this section, it can be assumed that a superposition of result entries has occurred.

Table 5: Results description index

Error term	Symbol
Leader to first follower	$e_{0,1}$
First follower to second follower	$e_{1,2}$
Second follower to third follower	$e_{2,3}$
Third follower to fourth follower	$e_{3,4}$
Fourth follower to fifth follower	$e_{4,5}$
Maximum distance between pair of followers	$\Delta_{x,\max}$
Minimum distance between pair of followers	$\Delta_{x,\min}$
Maximum velocity error between pair of followers	$\Delta_{v,\max}$
Minimum velocity error between pair of followers	$\Delta_{v,\min}$
Maximum acceleration error between pair of followers	$\Delta_{a,\max}$
Minimum acceleration error between pair of followers	$\Delta_{a,\min}$
Mean velocity error	χ_x
Mean acceleration error	χ_v
Mean position error	χ_a
Standard deviation position	Λ_x
Standard deviation velocity	Λ_v
Standard deviation acceleration	Λ_a
Position variance	Γ_x
Velocity variance	Γ_v
Acceleration variance	Γ_a

6.1.1 PD control strategy

6.1.1.1 Linear vehicle model

6.1.1.1.1 Inter-vehicular distance error

Consider Figure 12 below were the distance mismatch between platoon vehicles is represented. During all the constant velocity stages of the trapezoid manoeuvre from $t = 0 \leq t \leq 290\ s$, the distance mismatch between platoon followers and the lead vehicle is negligible. Over the same duration, during the vehicle acceleration and deceleration stages of the manoeuvre, the relative distance error between the lead and following vehicle becomes apparent. There is an estimated initial maximum inter-vehicular

distance error occurs between $e_{4,5}$ with a numerical value of $-150\ cm$ with respect to the lead vehicle during the time span mentioned above which occurs at $t = 210\ s$. The maximum rate of change in error $\Delta_{x,\max}$ between any pair of vehicles at the same time span is $50\ cm$ between $e_{3,4}$ and $e_{4,5}$. The minimum amount of inter-vehicular distance during the same time span mentioned above occurs between $e_{1,2}$ at $t = 25\ s$ which is observed to be about $25\ cm$. The minimum rate of change in error $\Delta_{x,\min}$ between any pair of vehicles at the same period is $10\ cm$ between $e_{3,4}$ and $e_{4,5}$.

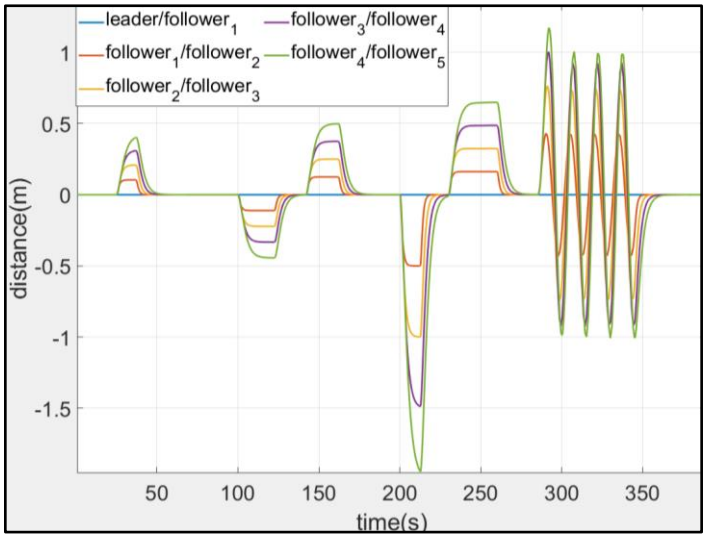

Figure 12: Inter-vehicular distance error for linear vehicle model for normal and emergency vehicle manoeuvre

During the emergency vehicle manoeuvre from $290 \leq t \leq 360\ s$ the maximum inter-vehicular distance error is observed at $e_{4,5}$ at $t = 290\ s$, the magnitude of the error is $130\ cm$. The maximum rate of change in error $\Delta_{x,\max}$ between any pair of vehicles during the manoeuver is $25\ cm$ between $e_{3,4}$ and $e_{4,5}$. The minimum amount of inter-vehicular distance during the manoeuvre mentioned above occurs between $e_{1,2}$ at $t = 325\ s$ which is observed to be about $40\ cm$. The minimum rate of change in error $\Delta_{x,\min}$ between any pair of vehicles at the same period is $5\ cm$ between $e_{3,4}$ and $e_{4,5}$. At the termination point of the manoeuvre, all vehicles in the platoon converge towards the trajectory of the leader at $360 \geq t \geq \infty$. Consequently, a conclusion can be made that the PD control structure is capable of bounding the inter-vehicular distance of a platoon according to 3.2 in steady state for vehicles with linear dynamics as in 3.7.

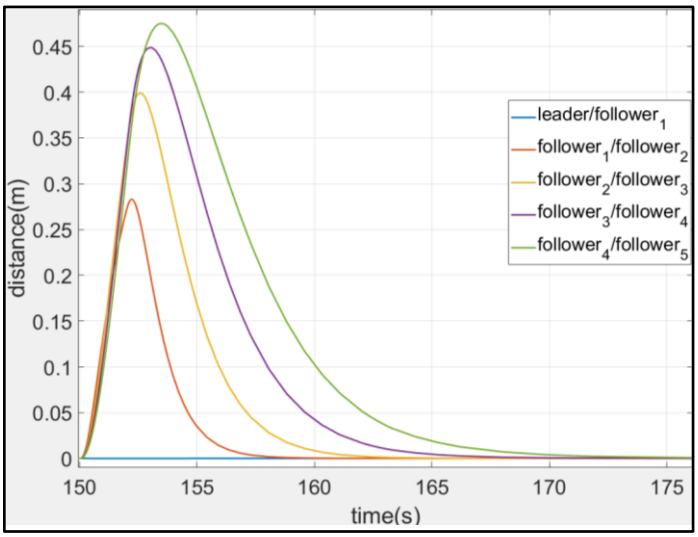

Figure 13: Inter-vehicular distance error for door function manoeuvre

Figure 13 shown above depicts the inter-vehicular distance error for the door function manoeuvre. The maximum inter-vehicular distance error in relation to the lead vehicle of 48 cm occurs between $e_{4,5}$ at $t = 155\ s$. It is noted that the maximum rate of change in error $\Delta_{x,\max}$ between any pair of vehicles are observed between $e_{2,3}$ and $e_{1,2}$ to be 12 cm. The minimum inter-vehicular distance error in concerning the lead vehicle is observed at $e_{1,2}$ to be 28 cm occurs at $t = 152\ s$. The minimum rate of change in error $\Delta_{x,\min}$ between any pair of vehicles at the same period is 3 cm between $e_{3,4}$ and $e_{4,5}$. It is noted that all platoon vehicles converge towards the trajectory of the leader gradually in steady state at $173 \leq t \leq \infty$.

6.1.1.1.2 Velocity response error

Represented in Figure 14 is relative velocity error between vehicle platoon followers. During all the constant velocity stages of the trapezoid manoeuvre from $t = 0 \leq t \leq 290\ s$, the velocity error between platoon followers and the lead vehicle is negligible. The maximum velocity error during the normal braking manoeuvre in relation $e_{0,1}$ is observed at $210 \leq t \leq 200\ s$ at $e_{4,5}$ with a numerical value of 0.3 km/hr. It is also observed that the maximum relative velocity error $\Delta_{v,\max}$ between any pair of vehicles $e_{3,4}$ and $e_{4,5}$ is negligible. Consequently, the lowest relative distance for the manoeuvre is $\Delta_{v,\min}$ is also deemed to be minimal.

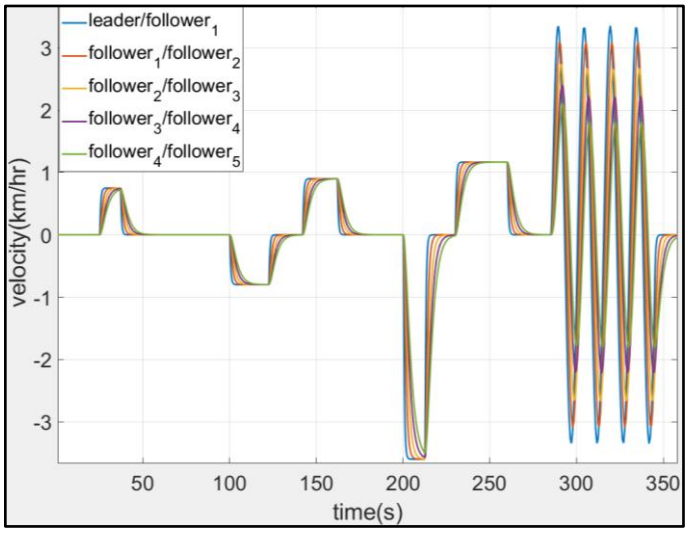

Figure 14: Relative velocity error between platoon vehicles for linear vehicle model for normal and emergency vehicle manoeuvre

During the emergency manoeuvre the maximum velocity error considering $e_{0,1}$ is $e_{4,5}$ observed between $290 \leq t \leq 340\ s$. The maximum relative velocity mismatch during the emergency manoeuvre $\Delta_{v,\max}$ between any pair of vehicles $e_{2,3}$ and $e_{3,4}$ is 0.3 km/hr and 0.3 km/hr over the same duration. The minimal relative distance error $\Delta_{v,\min}$ between any pair of vehicles $e_{3,4}$ and $e_{4,5}$ is 0.1 km/hr and $-0.1\ km/hr$ over the same duration. At the end of the manoeuvre, all vehicles converge towards the trajectory of the leader at time $360 \geq t \geq \infty$. As such the PD controller can bound the relative velocity error of according to 3.1 to a reasonable value for vehicles with linear dynamical models.

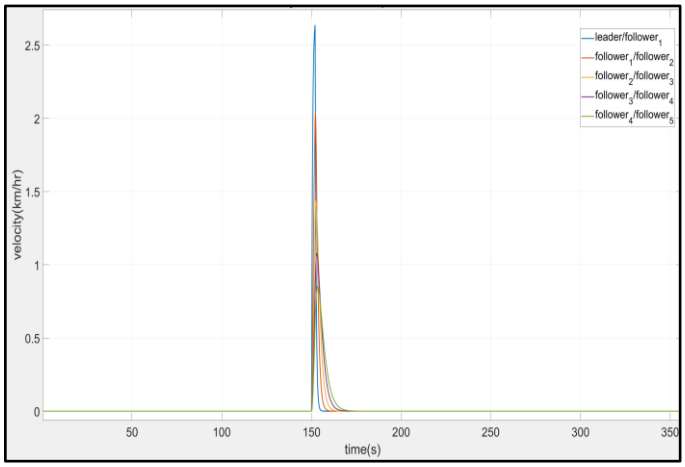

Figure 15: Relative vehicle velocity error for door function manoeuvre

Consider Figure 15 where the relative velocity error for the door function manoeuvre is highlighted. The initial transient of the system is stable from $0 \leq t \leq 150\ s$. This is expected as this represents the initial constantly velocity stage of the manoeuvre. The maximum relative velocity error between any pair of vehicles of $0.5\ km/hr$ is observed between $e_{0,1}$ and $e_{1,2}$ at $t = 152\ s$. This expected as this the peak of the acceleration stage of the manoeuvre. The minimum inter-vehicular distance between any pair of vehicles of $0.3\ km/hr$ occurs between $e_{3,4}$ and $e_{4,5}$ at the same time juncture mentioned above. Finally, at steady state, all platoon followers converge towards the trajectory of the lead vehicle as expected from the manoeuvre.

6.1.1.1.3 Acceleration response error

Represented in Figure 16 is relative acceleration error between platoon followers. During the initial normal braking manoeuvre, the constant velocity stage of the manoeuvre is stable, whilst a significant overshoot is observed at trapezoid stages of the manoeuvre all of which occur between $0 \leq t \leq 290\ s$. The maximum acceleration error occurs at $e_{0,1}$ is observed at $t = 200\ s$, the magnitude of this error is $0.14\ g$. The maximum acceleration error between any pair of vehicles $\Delta_{a,\max}$ occurs between $e_{l,1}$ and $e_{1,2}$ is $0.09\ g$. The least amount of acceleration error for the manoeuvre occurs at $e_{4,5}$ at $t = 40\ s$, the numerical value of this error is $-0.025\ g$. The minimum acceleration error between any pair of vehicles $\Delta_{a,\min}$ occurs between $e_{3,4}$ and $e_{4,5}$ is negligible.

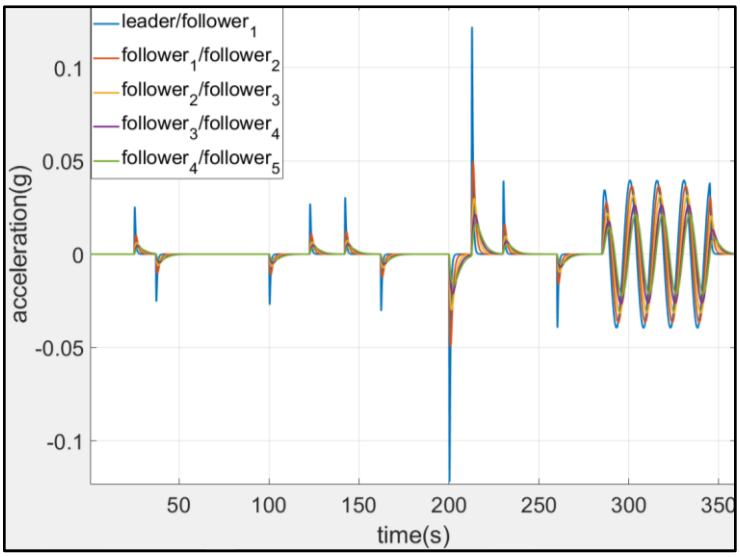

Figure 16: Relative acceleration error between platoon vehicles for linear vehicle model for normal and emergency vehicle manoeuvre

During the emergency manoeuvre between $290 \leq t \leq 340\ s$, the maximum acceleration error is at $e_{l,1}$ which is observed at $t = 290\ s$, the numerical value of this error is $0.038\ g$. The maximum acceleration error between any pair of vehicles $\Delta_{a,\max}$ occurs between $e_{0,1}$ and $e_{1,2}$ is $0.02\ g$. The least amount of acceleration error for the manoeuvre occurs at $e_{4,5}$ at $t = 290\ s$, the numerical value of this error is $0.02\ g$. The minimum acceleration error between any pair of vehicles $\Delta_{a,\min}$ occurs between $e_{3,4}$ and $e_{4,5}$ is negligible. At the end of the manoeuvre in steady state, all platoon followers converge towards the leader trajectory at $360 \leq t \leq \infty\ s$, as such can be regarded as stable.

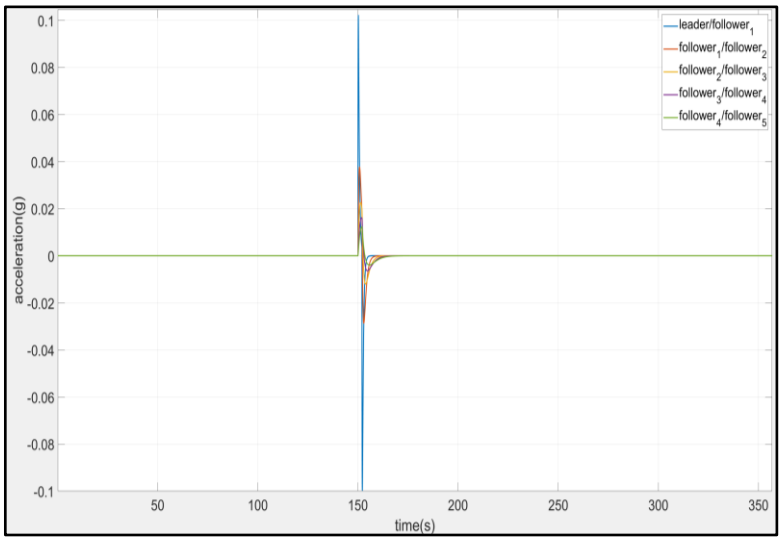

Figure 17: Relative vehicle acceleration error for door function manoeuvre

Consider Figure 17 where the relative acceleration error for the door function manoeuvre is illustrated. The initial transient of the system is stable from $0 \leq t \leq 150\ s$, and this is expected as it represents the initial constantly velocity stage of the manoeuvre. The maximum acceleration error between any pair of vehicles occurs $0.12\ g$ was observed between $e_{0,1}$ at $t = 152\ s$. This is expected as this occurs during the acceleration stage of the manoeuvre. The minimum acceleration error between any pair of vehicles of $-0.009\ g$ was observed between $e_{4,5}$ at $t = 155\ s$. In steady state at $160 \leq t \leq \infty\ s$ all the vehicles in the platoon converge towards the leader's trajectory.

6.1.1.2 Non-linear vehicle model limitation

6.1.1.2.1 Inter-vehicular distance error

Consider Figure 18 where initially at $t = 0\ s$ the distance mismatch between any pair of followers within the platoon is negligible. Progressively at $t > 0\ s$ the trajectory of pair of vehicle $e_{1,2}$ diverges away from the lead vehicle. The maximum error between a pair of vehicles under normal braking occurred at time $t = 225\ s$ was $-200\ cm$. This occurred between a pair of vehicles $e_{4,5}$. The maximum inter-vehicular distance during the emergency manoeuver occurred at the first peak of the first sinusoid at $t = 280\ s$ where the distance error is $100\ cm$ between pair of vehicles $e_{4,5}$.

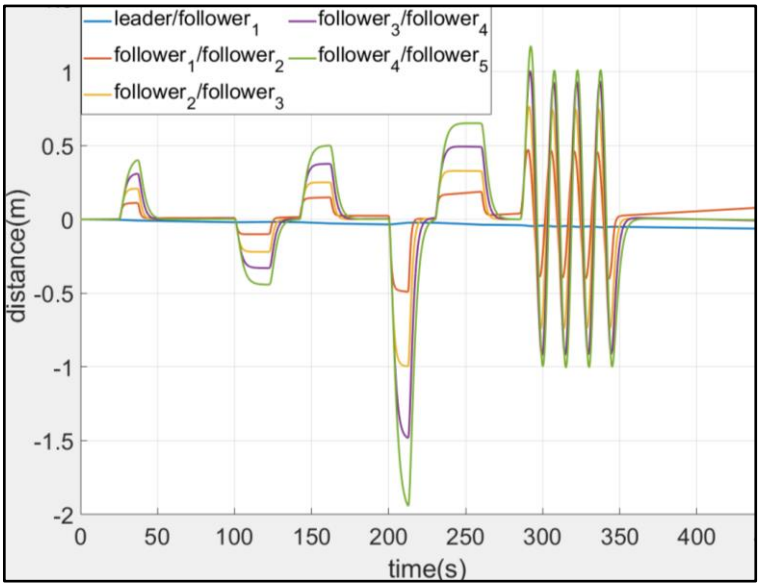

Figure 18: Inter-vehicular distance error for non-linear vehicle model for normal and emergency vehicle manoeuvre

At the termination point of the manoeuvre the relative error $e_{2,3}, e_{3,4}$and $e_{4,5}$ all get to steady state at $t > 360\ s$ with respect to the lead vehicle with a constant error of $100\ cm$. The relative error $e_{1,2}$ shows that a divergence might occur between the first and lead vehicle. Although, it is not possible to determine this fact because the simulation time is insufficient. As such it is noted that a collision will not occur at $t = \infty\ s$ as the first follower diverges away from the leader. Consequently, a conclusion can be made that the PD control structure is incapable of bounding the inter-vehicular distance in a platoon according to 3.2 with minimal error between vehicles with non-linear dynamics as in 3.4.

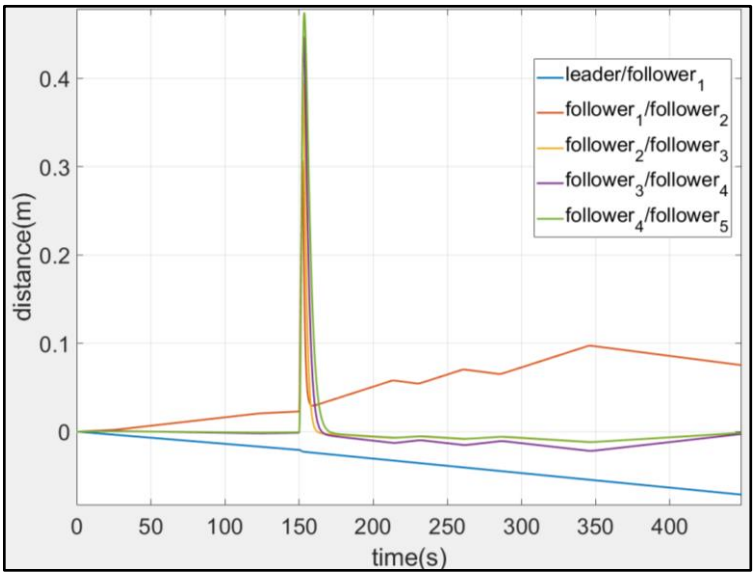

Figure 19: Inter-vehicular distance error for non-linear vehicle model for door manoeuvre

Consider Figure 19 where the relative inter-vehicular distance error for the door function manoeuvre is depicted. Initially, at the beginning of the manoeuvre at $0 \leq t \leq 150\ s$ it is highlighted that the error between the pair of vehicles $e_{1,2}$ diverge away from the trajectory of the first a pair of vehicles $e_{0,1}$. It is noted that this behaviour is not expected from the aforementioned vehicle manoeuvre. At the acceleration stage of the manoeuvre, it is noted that pair of vehicles $e_{2,3}$, $e_{3,4}$, and $e_{4,5}$ all begin to diverge away from $e_{1,2}$ from $150 \leq t \leq 345\ s$. From $345 \leq \infty$ inter-vehicular error $e_{2,3}$, $e_{3,4}$, and $e_{4,5}$ begin to converge towards the trajectory of $e_{1,2}$, although all followers still diverge away from the

trajectory of the leader. Consequently, a conclusion can also be deducted that $e_{0,1}$ is diverging hence likely to be reversing. Finally, it is noted that the exact behaviour of the platoon at $t = \infty\ s$ is unknown without a longer simulation time.

The PD controller can facilitate all platoon control objectives for the linear vehicle model although unable to provide the same requirements for the non-linear vehicle model as mentioned above. As such, the FA control strategy mentioned in 4.11 would be used to evaluate the non-linear vehicle model facilitate the platoon control objective mentioned in 3.1 and 3.2. It is noted that the controller was able to keep both the relative velocity and acceleration profiles respectively bounded with minimal error. For brevity, this is not included within the text of this document as such these evaluations are shown in the Appendix of this document.

It is noted that all the evaluations made this section were also carried for a homogenous platoon of 5 vehicles thus the results are highlighted in Appendices 1 to 6. It is also worth noting that these results were not included within the body of this document. It is common among literature that a controller capable of facilitating heterogeneous platoon objectives should be able to do the same for homogenous platoons. (Wu et al., 2016). Finally, a conclusion is made that the results shown in Figure 15 and Figure 22 from the heterogeneous platoon evaluation were identical to the homogenous results.

6.1.2 Adaptive control strategy

The FA control strategy was evaluated based on the structure mentioned in 4.11. Firstly, the capability of the controller to enhance significantly the results presented in Table 6 would be investigated. Furthermore, the ability of the strategy mentioned in 4.19 to bound the growth of adaptive gains is depicted. Consequently, the ability of the entries of the adjacency matrix mentioned in chapter 3 to converge to dynamics of stable equilibria is shown. It is noted that the controller is only tested for non-linear vehicle dynamics for brevity.

6.1.2.1 Inter-vehicular distance

Consider Figure 20 below were the distance mismatch between platoon vehicles is represented. During all the constant velocity stages of the trapezoid manoeuvre such that $0 \leq t \leq 290\ s$, the distance mismatch between platoon followers and the lead vehicle is negligible. Over the same duration, during the vehicle acceleration and deceleration stages of the manoeuvre, the relative distance error between the lead and following vehicle becomes apparent. There is an estimated initial maximum inter-vehicular distance error occurs between $e_{4,5}$ with a numerical value of $11\ cm$ considering the lead vehicle during the time span mentioned above which occurs at $t = 27\ s$. The maximum rate of change in error $\Delta_{x,\max}$ between any pair of vehicles during the manoeuver is $66\ cm$ between $e_{2,3}$ and $e_{4,5}$. The minimum amount of inter-vehicular distance during the same time span mentioned above occurs between at $t = 27\ s$ which is observed to be about $-58\ cm$ and $58\ cm$ respectively. The minimum rate of change in error $\Delta_{x,\min}$ between any pair of vehicles at the same period is negligible between $e_{3,4}$ and $e_{4,5}$.

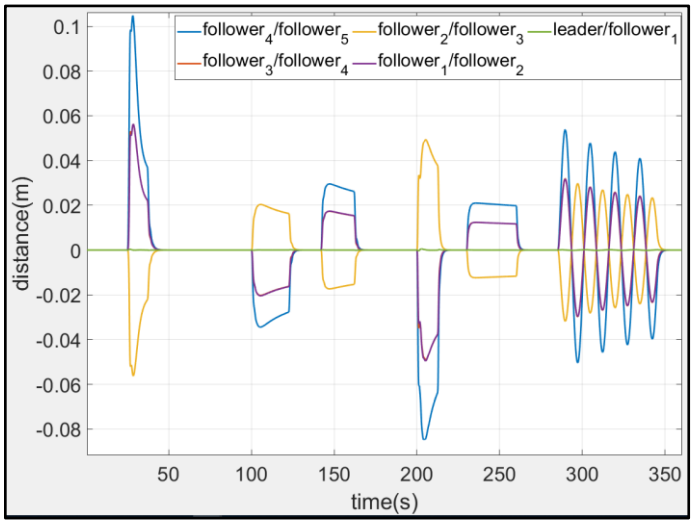

Figure 20: Inter-vehicular distance error for FA controller under normal and emergency braking

During the emergency vehicle manoeuvre from $290 \leq t \leq 360\ s$ the maximum inter-vehicular distance error is observed at $e_{4,5}$ at $t = 290\ s$, the magnitude of the error is $58\ cm$. The maximum error $\Delta_{x,\max}$ between any pair of vehicles during the manoeuvre is $20\ cm$ between $e_{3,4}$ and $e_{4,5}$. The minimum amount of inter-vehicular distance during the manoeuvre mentioned above occurs at $e_{1,2}$ at $t = 325\ s$ which is observed to be about $2\ cm$. The minimum rate of change in error $\Delta_{x,\min}$ between any pair of vehicles at the same time span is negligible between $e_{3,4}$ and $e_{2,3}$. At the termination point of the manoeuvre all vehicles in the platoon converge towards the trajectory of the leader at $360 \geq t \geq \infty$. Consequently, a conclusion can be made that the FA control strategy is capable of bounding the inter-vehicular distance in a platoon according to 3.2 in steady state for vehicles with non-linear dynamics as in 3.7.

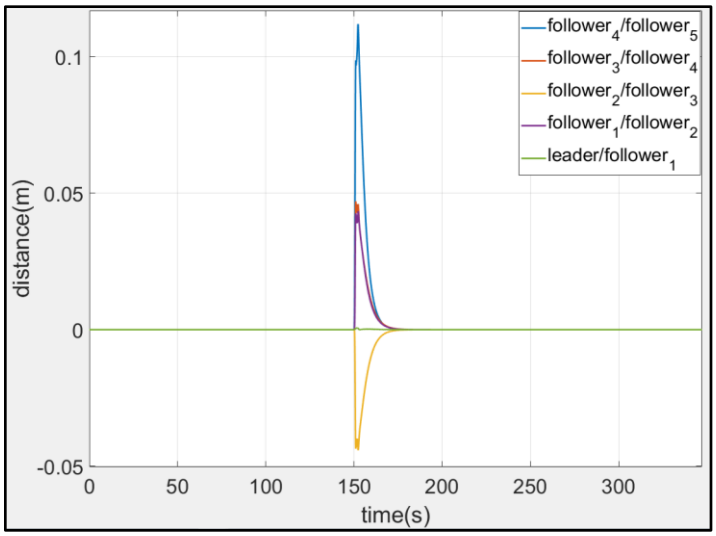

Figure 21: Inter-vehicular distance error for FA controller for door function manoeuvre

Figure 21 shown above depicts the inter-vehicular distance error for the door function manoeuvre. The maximum inter-vehicular distance error in relation to the lead vehicle of $18\ cm$ occurs between $e_{4,5}$ at $t = 152\ s$. It is noted that the maximum error $\Delta_{x,\max}$ between any pair of vehicles are observed between $e_{4,5}$ and $e_{1,2}$ to be $12\ cm$ during the acceleration manoeuvre. The minimum inter-vehicular distance error considering the lead vehicle is observed is $4.8\ cm$ and $-4.8\ cm$ occurs at $t = 152\ s$. The minimum rate of change in error $\Delta_{x,\min}$ between any pair of vehicles at the same period is cm between $e_{3,4}$ and $e_{2,3}$ is negligible. It is noted that all platoon vehicles converge towards the trajectory of the leader gradually in steady state at $173 \leq t \leq \infty$.

6.1.2.2 Velocity response error

Represented in Figure 22 is the relative velocity error between vehicle platoon followers. During all the constant velocity stages of the trapezoid manoeuvre from $t = 0 - 290\ s$, the velocity error between platoon followers and the lead vehicle is negligible. The maximum velocity error during the normal braking manoeuvre in relation $e_{0,1}$ is observed at $210 \leq t \leq 200\ s$ at $e_{4,5}$ which has a numerical value of $0.52\ km/hr$ and $-0.52\ km/hr$. It is observed that the maximum relative velocity error $\Delta_{v,\max}$ between any pair of vehicles $e_{3,4}$ and $e_{4,5}$ is $0.4\ km/hr$ at $t = 200\ s$. Consequently, the lowest relative distance for the manoeuvre is $\Delta_{v,\min}$ is also deemed to be minimal.

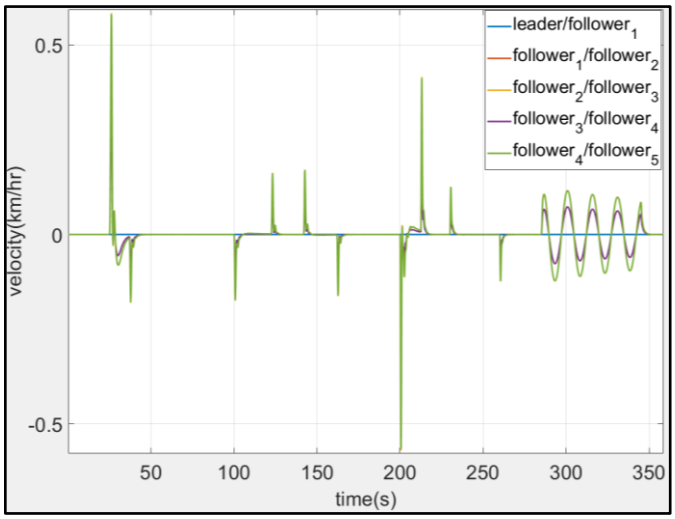

Figure 22: Relative velocity error under normal and emergency braking

During the emergency manoeuvre the maximum velocity error in relation to $e_{0,1}$ is $e_{4,5}$ observed between $t = 340\ s$ is $0.1\ km/hr$. The maximum relative velocity mismatch during the emergency manoeuvre $\Delta_{v,\max}$ between any pair of vehicles $e_{4,5}$ and $e_{3,4}$ is $0.043\ km/hr$. The minimum velocity $e_{1,2}$ error during the manoeuver is $0.054\ km/hr$ during the same time span. The minimal relative distance error $\Delta_{v,\min}$ between any pair of vehicles $e_{3,4}$ and $e_{4,5}$ is negligible. Over the same duration. At the end of the manoeuvre, all vehicles converge towards the trajectory of the leader at time $360 \geq t \geq \infty$. As such the FA controller is able to bound the relative velocity error of the platoon according to 3.2 for non-linear vehicle models.

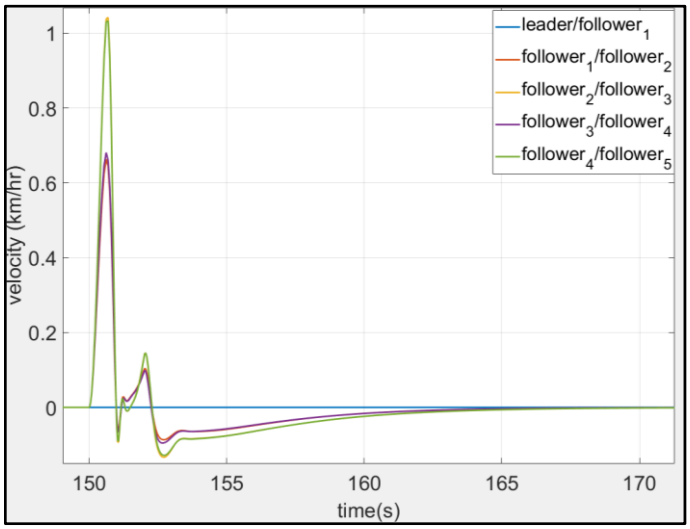

Figure 23: Relative velocity error for FA controller during door function manoeuvre

Consider Figure 23 where the relative velocity error for the door function manoeuvre is highlighted. The initial transient of the system is stable from $0 \leq t \leq 150\ s$, this is expected as this represents the initial constant velocity stage of the manoeuvre. The maximum relative velocity error between any pair of vehicles of $1.2\ km/hr$ is observed between $e_{0,1}$ and $e_{4,5}$ at $t = 152\ s$. This expected as this the peak of the acceleration stage of the manoeuvre. The minimum inter-vehicular distance between any pair of vehicles of $0.08\ km/hr$ occurs between $e_{3,4}$ and $e_{4,5}$ at $t = 154\ s$. Finally, at $t = 164\ s$ all platoon followers converge towards the trajectory of the lead vehicle as expected from the manoeuvre.

6.1.2.3 Acceleration response error

Represented in Figure 24 is the relative acceleration error between platoon followers. During the initial normal braking manoeuvre, the constant velocity stage of the manoeuvre is stable, whilst a significant overshoot is observed at trapezoid stages of the manoeuvre all of which occur between $0 \leq t \leq 290\ s$. The maximum acceleration error occurs at $e_{0,1}$ is observed at $t = 200\ s$, the magnitude of this error is $-0.042\ g$. The maximum acceleration error between any pair of vehicles $\Delta_{a,\max}$ occurs between $e_{l,1}$ and $e_{1,2}$ is negligible. The least amount of acceleration error for the manoeuvre occurs at $e_{4,5}$ at $t = 40\ s$, the numerical value of this error is $0.0009\ g$. The minimum acceleration error between any pair of vehicles $\Delta_{a,\min}$ occurs between $e_{3,4}$ and $e_{4,5}$ is negligible.

During the emergency manoeuvre between $290 \leq t \leq 340\ s$, the maximum acceleration error is at $e_{0,1}$ which is observed at $t = 290\ s$, the numerical value of this error is $0.0005\ g$. The maximum acceleration error between any pair of vehicles $\Delta_{a,\max}$ occurs between $e_{0,1}$ and $e_{1,2}$ is $0.0002\ g$. The least amount of acceleration error for the manoeuvre occurs at $e_{4,5}$ at $t = 290\ s$, the numerical value of this error is negligible. The minimum acceleration error between any pair of vehicles $\Delta_{a,\min}$ occurs between $e_{3,4}$ and $e_{4,5}$ is negligible. At the end of the manoeuvre all platoon followers converge towards the leader trajectory at $360 \leq t \leq \infty\ s$, as such can be considered as stable.

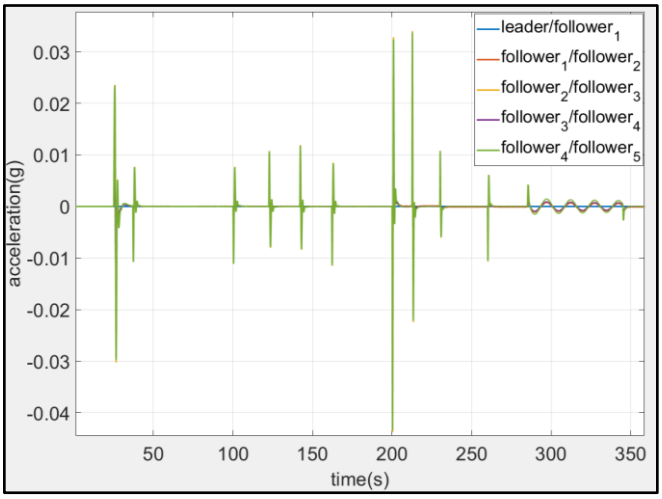

Figure 24: Relative acceleration for FA controller under normal and emergency manoeuvre

Consider Figure 25 where the relative acceleration error for the door function manoeuvre is illustrated. The initial transient of the system is stable from $0 \leq t \leq 150\ s$, this is expected as this represents the initial constantly velocity stage of the manoeuvre. The maximum acceleration error between any pair of vehicles occurs $0.12\ g$ was observed between $e_{0,1}$ at $t = 152\ s$. This is expected as this occurs during the acceleration stage of the manoeuvre. The minimum acceleration error between any pair of vehicles of $-0.009\ g$ was observed between $e_{4,5}$ at $t = 155\ s$. At $160 \leq t \leq \infty\ s$ all the vehicles in the platoon converge towards the leader's trajectory.

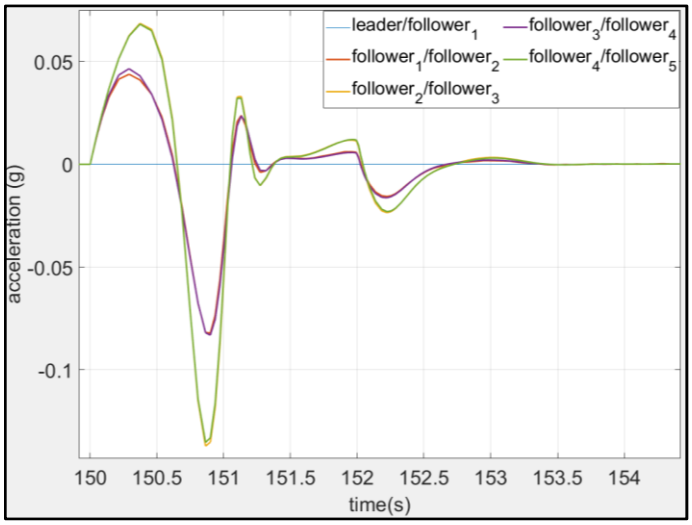

Figure 25: Relative velocity error for FA controller during door function manoeuvre

6.1.2.4 Evolution of adaptive gains and entries of the adjacency matrix

This section is dedicated to outlining the evolution of adaptive gains for both fixed and adaptive topologies respectively. These results highlight the evolution of adaptive gains between the lead vehicle and any generic follower $K_{0,i}$. Consequently the evolution of gains from one generic follower to another K_{ij} is also investigated. Furthermore, the dynamical entry of the adjacency matrix from follower to follower A_{N+1} is also depicted.

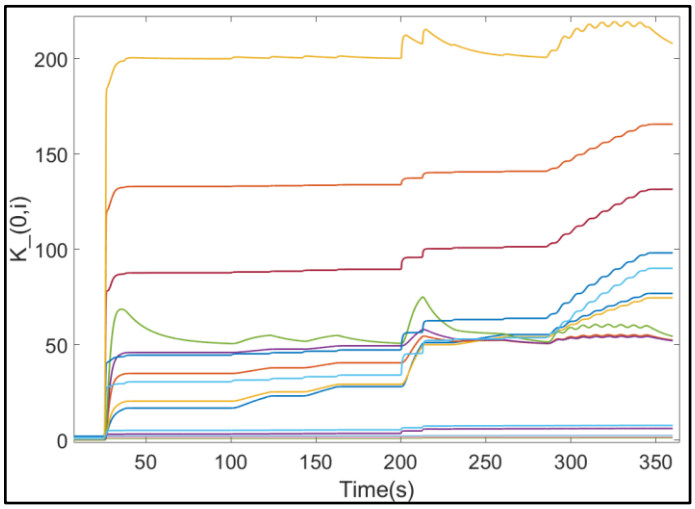

Figure 26: Evolution of adaptive gains from leader to followers

Outlined in Figure 26 is the evolution of the adaptive control gains for the leader to follower topology, all gains are bounded and converge towards a constant value. It is noted that the control gains for each state are depicted for each state within the diagram, this was done for brevity. It is noted that the σ-modification technique mentioned in 4.21 is activated thus used to bound the increasing trend of some adaptive gains.

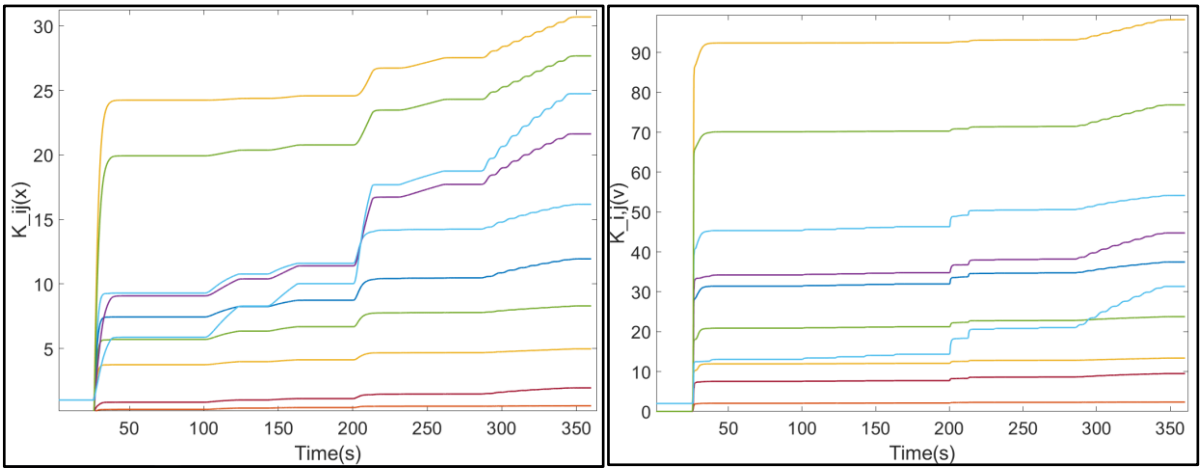

Figure 27: Evolution of position gains from follower to follower for position and velocity

Outlined in Figure 27 and Figure 28 is the evolution of the adaptive position and velocity control gains of follower to follower topology, all gains are bounded and converge towards a constant value. The gains of the position adaptive gains converge to a maximum value of 30 while the control gains of the velocity adaptive gains converge to a maximum value of 95. It is pointed out that the strategy mentioned in 4.19 activates hence prevents the unbounded drift of control gains. Consequently, it is noted that the tuning of the maximum and minimum convergence value of the adaptive gains is a trivial process. Furthermore since the vehicle states in Figure 27 and Figure 28 are bounded and controller gains are bounded, the control actions are consequently bounded.

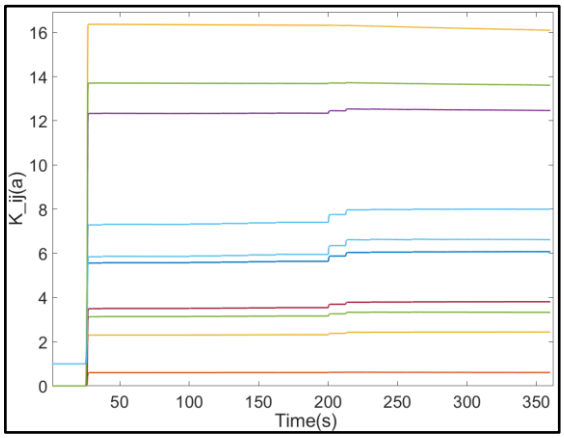

Figure 28: Evolution of acceleration adaptive gains from follower to follower

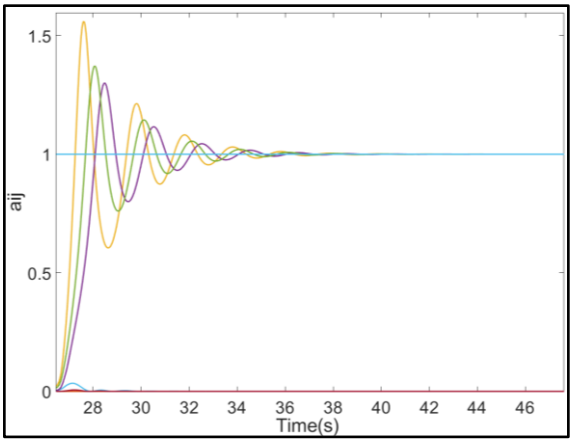

Figure 29: Entries of the adjacency matrix from follower to follower A_{N+1}

As highlighted in chapter 4 of this document, the potential field depicted in Figure 8 imposes two stable equilibria 0 and 1 respectively. This is in conjunction with the second order system mentioned in 4.14 which depicts the dynamics of the entries of the adjacency matrix $A_{N+1}$of G_{N+1}. This phenomenon is represented in Figure 30 where the entries of the adjacency A_{N+1} are represented. The arcs of the equivalent adjacency matrix that converges to 0 is excluded from the initial all-to-all topology on the left and yields a new platoon topology in steady state shown on the right. It is noted that the topology illustrated in on the left has 25 arcs while the new topology on the right has 13 arcs hence the links of the network are reduced by 48% thereby mitigating the load on the network and alleviating network communication issues such as latency and packet loss.

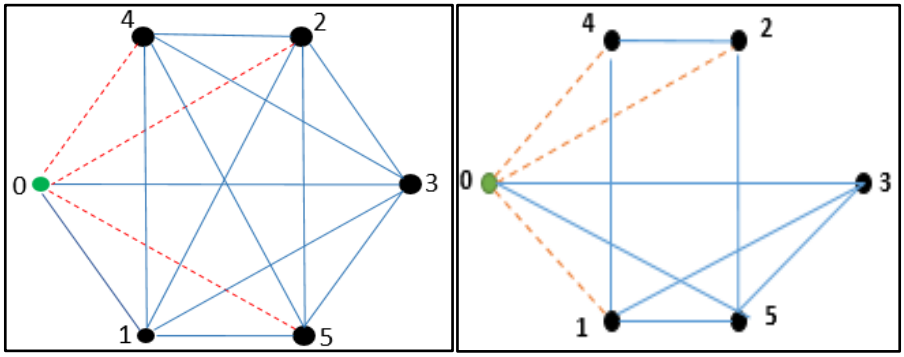

Figure 30: Initial all-to-all platoon network topology (on the left) and emerging topology (on the right)

For the purposes of this project, the topology between follower vehicles will be considered to be a BD type all-to-all topology as in Figure 5. Outlined in 6.1 is the depiction of the adjacency matrix which represents the topology mentioned above. As outlined in chapter 4 of this document, where 1 represents a link between two generic platoon vehicles and 0 otherwise represents no link between the vehicles. For the topology between the lead vehicle and corresponding followers, the topology is such that $K_{0,1}$ and $K_{0,3}$ are fixed while $K_{0,2}$, $K_{0,4}$, and $K_{0,5}$ are adaptive. This phenomenon is illustrated in Figure 30 where the dotted orange lines represent adaptive links while solid blue lines represent fixed links in the network. Where the lead vehicle is represented by a green circle and corresponding followers are outlined by black ones. It is noted that Figure 30 only portrays the position of vehicles on the graphical network mentioned in chapter 3 and not the positions of the vehicle on the road.

$$A_{N+1} = \begin{matrix} 0 & 0 & 1 & 1 & 1 \\ 0 & 0 & 0 & 1 & 1 \\ 1 & 0 & 0 & 0 & 1 \\ 1 & 1 & 0 & 0 & 0 \\ 1 & 1 & 1 & 0 & 0 \end{matrix} \qquad 6.1$$

6.2 Controller performance index

This section is devoted to carrying out a quantitative comparison of the control strategies analysed within this chapter. For brevity, the ability of both controllers to facilitate platooning objectives would be evaluated based on three KPIs which are the mean, standard deviation, and variance. This would be done for all two major vehicle manoeuvres evaluated in this report. For the sake of brevity all comparisons related to the normal braking manoeuvre would be done at $t = 200\ s$. Consequently all analysis carried out on both the emergency braking manoeuvre and door function manoeuvre would be done at $t = 290\ s$ and $t = 152\ s$ repectively. It is noted that the plots included in this section are not limited to the durations mentioned above.

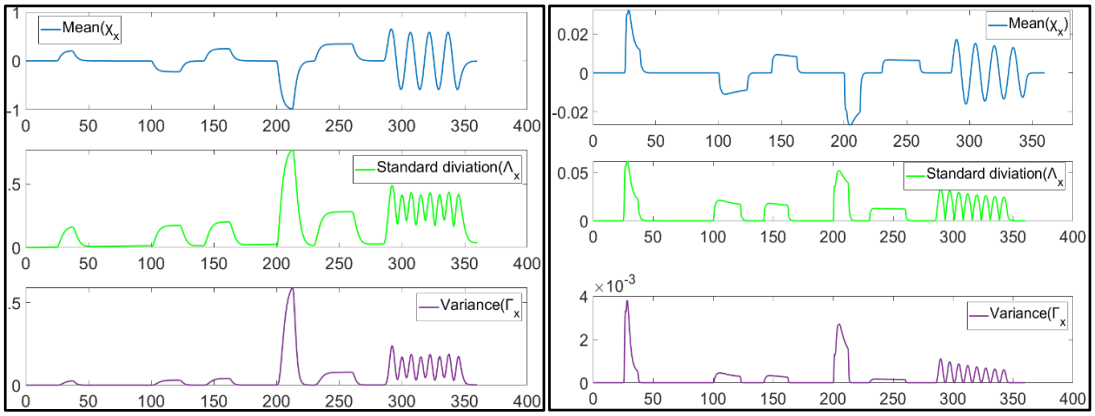

Figure 31: Position KPIs for FA and PD normal and emergency braking

Illustrated in Figure 31 respectively are the inter-vehicular distance KPIs for both the PD and FA control strategy respectively. The mean inter-vehicular error of the FA controller is 98% more effective than that of the PD controller. Finally, the inter-vehicular error variance of the FA controller is also characterized by 99% enhancement on the PD controller results. Represented in Figure 32 Respectively are the velocity profile KPIs for both the PD and FA control strategy respectively. The mean velocity profile of the FA controller is exactly the same as that of the PD controller. Finally, the velocity variance of the FA controller is also characterized by approximately 100% enhancement on the PD controller results**.**

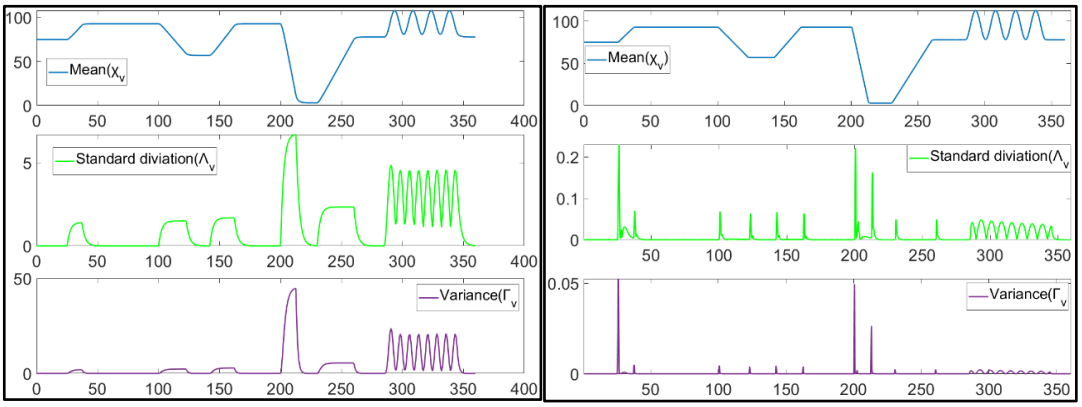

Figure 32: Velocity KPIs for FA and PD normal and emergency braking

Highlighted in Figure 33 respectively are the acceleration profile KPIs for both the PD and FA control strategy respectively. The mean acceleration profile of the FA controller is exactly the same as that of the PD controller. Finally, variance of the FA controller is also characterized by 95.8% enhancement on the PD controller results.

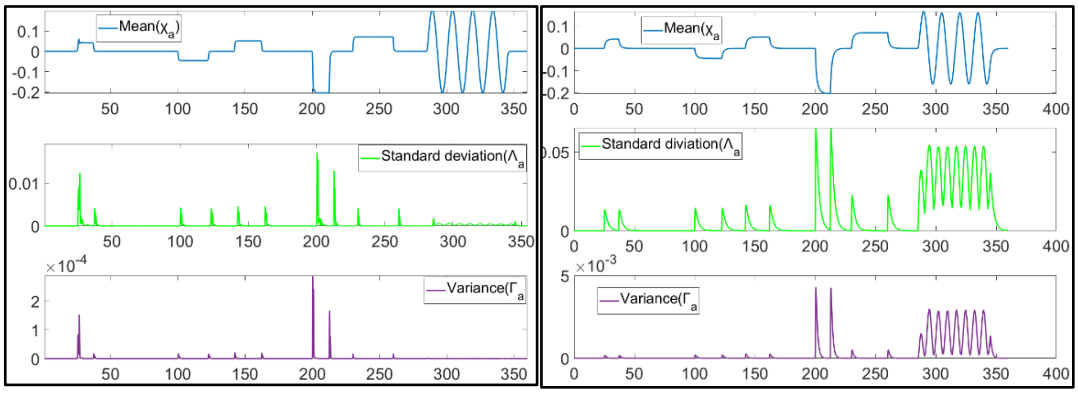

Figure 33: Acceleration KPIs for FA and PD normal and emergency braking

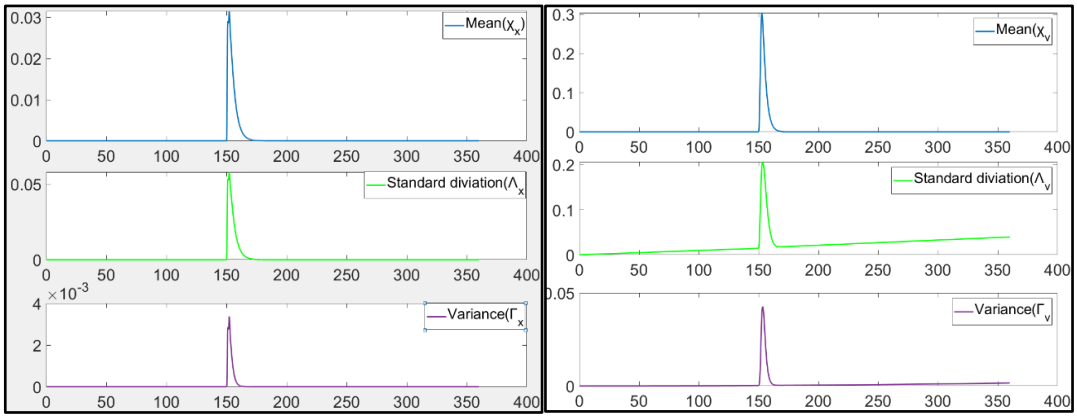

Figure 34: Inter-vehicular error profile KPIs for FA and PD door manoeuvre

Highlighted in Figure 35 respectively are the velocity profile KPIs for both the PD and FA control strategy respectively. The mean acceleration profile of the FA controller is exactly the same as that of the PD controller. Finally, variance of the FA controller is also characterized by 98.1% enhancement on the PD controller results. Highlighted in Figure 34 respectively are the inter-vehicular distance error KPIs for both the PD and FA control strategy respectively. The mean acceleration profile of the FA controller is exactly the same as that of the PD controller. Finally, variance of the FA controller is also characterized by 92.5% enhancement on the PD controller results.

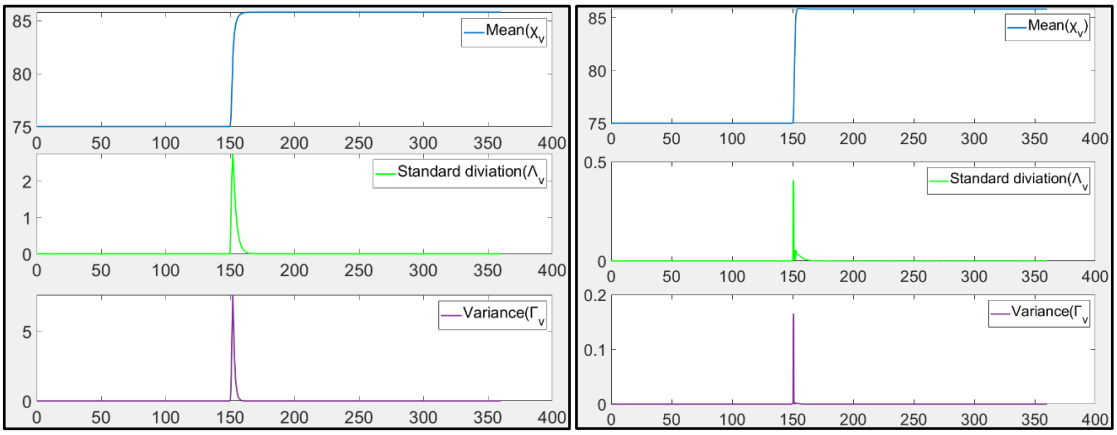

Figure 35: Velocity profile KPIs for FA and PD door manoeuvre

From the various analysis executed within this chapter, it has been proven beyond reasonable doubt that the FA control strategy is a quantitatively more effective controller for vehicle platooning. Furthermore this highlights the neccesity of a robust control algorithm to effectively execute the contol of autonomous vehicle platoons. As such it can be stated that the spread of the FA control strategy error results is negligible compared to the PD controller.

7. Concluding Remarks

7.1 Project conclusion

The economic and environmental incentive of vehicle platooning were explored through review of literature. The benefits and theoretical components of vehicle platooning were also explored through a literature review. This project has proven the limitations of a controller with fixed gain and fixed topology to facilitate platoon control requirements therefore showcased the necessity of implementing a robust control algorithm capable of facilitating these requirements with respect to network imperfections. Platoon control evaluation was done on a non-linear vehicle model. It is noted that controller evaluation done within this document excluded the mid-level controller hence mitigating the effectiveness of the feedback-linearization technique. As such the control law was exerted directly on the non-linear model.

The two control approaches investigated was a PD control strategy and an FA control strategy. Where the PD controller is the controller with fixed gain and fixed topology while the FA controller is the robust control algorithm with adaptive gain and adaptive topology. It is noted that the PD control structure was able provide platoon control objectives when considering linear vehicle dynamics. Furthermore, when the controller was implemented on a platoon with non-linear vehicle dynamics, this established that the followers diverged away from the trajectory of the lead vehicle. Finally, numerical results of the FA control strategy on non-linear platoon vehicles has proved its ability to create and maintain platoon formations notwithstanding of a velocity variation of the lead vehicle whilst adaptively selecting its network topology. As such, the controller was able to successfully guarantee platooning objectives for a non-linear vehicle model with minimal error despite the influence of network communication imperfections.

7.2 Further work

Despite the promising results of the project, being able showcase the functional operability of a robust control algorithm capable of ensuring platoon control objectives. Critical discussion topics still arise when considering the wider spectrum of platoon control mentioned in this document. These issues mainly gravitate towards the inability of the longitudinal vehicle model to depict realistic vehicle dynamics. For the longitudinal vehicle dynamics suggested areas of improvement include but are not limited to the inclusion of vehicle pitch and yaw, exact modelling of vehicle powertrain dynamics, and the inclusion of tire longitudinal slip in vehicle model. In a scenario where the project was not impeded by time constraints, further tests would have been ran towards establishing the limitations of the FA control strategy.

These might include the addition of more vehicles to platoon test scenario although it is noted that from the author's perspective that the consequence on control effectives would be minimal. Furthermore, it is expected that analysing platoon effectiveness with respect to different traffic scenarios might have yielded different results. The road surface was assumed to be smooth as such the effects of traffic road disturbances on the platoon were not investigated. It is then recommended that the control algorithm be tested on physical vehicle applications. The compatibility of the control algorithm with existing industry standard technologies such as ADAS is paramount to ensure collision avoidance, blind spot monitoring and the initiation of vehicle manoeuvres. It is also beneficial to understand the physical effects of communication platforms on the actual vehicle and its peripherals. All the above mentioned procedures would facilitate the ability of the control architecture to be potentially implemented on road vehicle successfully in separate traffic scenarios.

8. References

1. Alam, A., Besselink, B., Turri, V., Martensson, J. and Johansson, K. (2015). Heavy-Duty Vehicle Platooning for Sustainable Freight Transportation: A Cooperative Method to Enhance Safety and Efficiency. IEEE Control Systems, 35(6), pp.34-56.
2. Al Ridhawi, I., Aloqaily, M., Kotb, Y., Al Ridhawi, Y. and Jararweh, Y. (2018). A collaborative mobile edge computing and user solution for service composition in 5G systems. *Transactions on Emerging Telecommunications Technologies*, 29(11), p.e3446.
3. Aria, E., Olstam, J. and Schwietering, C. (2016). Investigation of Automated Vehicle Effects on Driver's Behavior and Traffic Performance. Transportation Research Procedia, [online] 15, pp.761-770.
4. Barooah, P., Mehta, P. and Hespanha, J. (2009). Mistuning-Based Control Design to Improve Closed-Loop Stability Margin of Vehicular Platoons. *IEEE Transactions on Automatic Control*, 54(9), pp.2100-2113.
5. Bu, F., Tan, S. and Huang, J. (2010). Nowakowski, C., O'Connell, J., Shladover, S. and Cody, D. (2010). Cooperative Adaptive Cruise Control: Driver Acceptance of Following Gap Settings Less than One Second. Proceedings of the Human Factors and Ergonomics Society Annual Meeting, 54(24), pp.2033-2037. PROC. ACC, pp.4616 - 4621.
6. Control issues in automated highway systems. (1994). *IEEE Control Systems*, 14(6), pp.21-32.
7. Darbha, S. and Pagilla, P. (2010). Limitations of employing undirected information flow graphs for the maintenance of rigid formations for heterogeneous vehicles. *International Journal of Engineering Science*, 48(11), pp.1164-1178.
8. Davila, A., Del Pozo, E., Aramburu, E. and Freixas, A. (2013). Environmental Benefits of Vehicle Platooning. SAE International. [online] Available at: https://saemobilus.sae.org/content/2013-26-0142 [Accessed 30 Oct. 2018].
9. DeLellis, P., di Bernardo, M. and Porfiri, M. (2011). Pinning control of complex networks via edge snapping. Chaos: An Interdisciplinary Journal of Nonlinear Science, 21(3), p.033119.
10. Eben Li, S., Li, K. and Wang, J. (2013). Economy-oriented vehicle adaptive cruise control with coordinating multiple objectives function. Vehicle System Dynamics, 51(1), pp.1-17.
11. Ferrara, A. and Vecchio, C. (2009). Second order sliding mode control of vehicles with distributed collision avoidance capabilities. *Mechatronics*, 19(4), pp.471-477.
12. Gamazo, A. (2013). RESEÑA de : EURYDICE. Key Data on Teachers and School Leaders in Europe : 2013 Edition. Luxembourg : Publications Office of the European Union, 2013. *Revista Española de Educación Comparada*, 0(22), p.235.
13. Ghasemi, A., Kazemi, R. and Azadi, S. (2013). Stable Decentralized Control of a Platoon of Vehicles With Heterogeneous Information Feedback. IEEE Transactions on Vehicular Technology, 62(9), pp.4299-4308.
14. Graham, L., Rideout, G., Rosenblatt, D. and Hendren, J. (2008). Greenhouse gas emissions from heavy-duty vehicles. *Atmospheric Environment*, 42(19), pp.4665-4681.
15. Guo, G. and Yue, W. (2012). Autonomous Platoon Control Allowing Range-Limited Sensors. *IEEE Transactions on Vehicular Technology*, 61(7), pp.2901-2912.
16. Ioannou PA. Automated highway systems. New York: Springer; 1997.
17. Harfouch, Y., Yuan, S. and Baldi, S. (2018). An Adaptive Switched Control Approach to Heterogeneous Platooning With Intervehicle Communication Losses. IEEE Transactions on Control of Network Systems, 5(3), pp.1434-1444.
18. Hobert, L., Festag, A., Llatser, I., Altomare, L., Visintainer, F. and Kovacs, A. (2015). Enhancements of V2X communication in support of cooperative autonomous driving. IEEE Communications Magazine, 53(12), pp.64-70.
19. Jain, A. (2018). vehicle to vehicle communication and Platooning. [online] Automotive Electronics. Available at: https://automotivelectronics.com/vehicle-to-vehicle-communication-and-platooning/ [Accessed 26 Dec. 2018].

20. Kianfar, R., Augusto, B., Ebadighajari, A., Hakeem, U., Nilsson, J., Raza, A., Tabar, R., Irukulapati, N., Englund, C., Falcone, P., Papanastasiou, S., Svensson, L. and Wymeersch, H. (2012). Design and Experimental Validation of a Cooperative Driving System in the Grand Cooperative Driving Challenge. IEEE Transactions on Intelligent Transportation Systems, 13(3), pp.994-1007.
21. Lari, M. (2018). Transmission delay minimization in wireless powered communication systems. Wireless Networks, 25(3), pp.1415-1430.
22. Lin, F., Fardad, M. and Jovanovic, M. (2013). Design of Optimal Sparse Feedback Gains via the Alternating Direction Method of Multipliers. *IEEE Transactions on Automatic Control*, 58(9), pp.2426-2431.
23. Li, S., Deng, K., Zheng, Y. and Peng, H. (2015). Effect of Pulse-and-Glide Strategy on Traffic Flow for a Platoon of Mixed Automated and Manually Driven Vehicles. *Computer-Aided Civil and Infrastructure Engineering*, 30(11), pp.892-905.
24. Li, S., Zheng, Y., Li, K., Wu, Y., Hedrick, J., Gao, F. and Zhang, H. (2017). Dynamical Modeling and Distributed Control of Connected and Automated Vehicles: Challenges and Opportunities. IEEE Intelligent Transportation Systems Magazine, 9(3), pp.46-58.
25. Li, S., Li, K., Rajamani, R. and Wang, J. (2011). Model Predictive Multi-Objective Vehicular Adaptive Cruise Control. IEEE Transactions on Control Systems Technology, 19(3), pp.556-566.
26. Li, S., Qin, X., Li, K., Wang, J. and Xie, B. (2017). Robustness Analysis and Controller Synthesis of Homogeneous Vehicular Platoons With Bounded Parameter Uncertainty. IEEE/ASME Transactions on Mechatronics, 22(2), pp.1014-1025.
27. Lochrane, T. (2015). cooperative adaptive cruise control - Google Search. [online] Google.com.:[Accessed 25 Dec. 2018].
28. Lygeros, J., Godbole, D. and Sastry, S. (1998). Verified hybrid controllers for automated vehicles. *IEEE Transactions on Automatic Control*, 43(4), pp.522-539.
29. Maschuw, J. and Abel, D. (2010). Longitudinal Vehicle Guidance in Networks with changing Communication Topology. IFAC Proceedings Volumes, 43(7), pp.785-790.
30. Milanes, V., Shladover, S., Spring, J., Nowakowski, C., Kawazoe, H. and Nakamura, M. (2014). Cooperative Adaptive Cruise Control in Real Traffic Situations. IEEE Transactions on Intelligent Transportation Systems, 15(1), pp.296-305.
31. Montanaro, U., Dixit, S., Fallah, S., Dianati, M., Stevens, A., Oxtoby, D. and Mouzakitis, A. (2018). Towards connected autonomous driving: review of use-cases. International Journal of Vehicle Mechanics and Mobility, [online] pp.4-9. Available at: https://www.tandfonline.com/loi/nvsd20 [Accessed 26 Nov. 2018].
32. Montanaro, U., Fallah, S., Dianati, M., Oxtoby, D., Mizutani, T. and Mouzakitis, A. (2018). On a fully self-organising vehicle platooning supported by cloud computing. Surrey Research Insight. [online] Available at: http://epubs.surrey.ac.uk/849285/ [Accessed 12 Oct. 2018].
33. Neophytou, V. (2016). Towards a Single European Maritime Transport Area: A Case of Expansion of the Internal Market. *SSRN Electronic Journal*.
34. Nowakowski, C., O'Connell, J., Shladover, S. and Cody, D. (2010). Cooperative Adaptive Cruise Control: Driver Acceptance of Following Gap Settings Less than One Second. Proceedings of the Human Factors and Ergonomics Society Annual Meeting, 54(24), pp.2033-2037.
35. NHTSA. National motor vehicle crash causation survey. U.S. Department of Transportation, National Highway Traffic Safety Administration; 2008.
36. Oncu, S., Ploeg, J., van de Wouw, N. and Nijmeijer, H. (2014). Cooperative Adaptive Cruise Control: Network-Aware Analysis of String Stability. IEEE Transactions on Intelligent Transportation Systems, [online] 15(4), pp.1527-1537. Available at: https://ieeexplore.ieee.org/document/6747309 [Accessed 15 Nov. 2018].
37. Ploeg, J., Shukla, D., van de Wouw, N. and Nijmeijer, H. (2014). Controller Synthesis for String Stability of Vehicle Platoons. *IEEE Transactions on Intelligent Transportation Systems*, 15(2), pp.854-865.

38. Petrillo, A., Salvi, A., Santini, S. and Valente, A. (2018). Adaptive multi-agents synchronization for collaborative driving of autonomous vehicles with multiple communication delays. Transportation Research Part C: Emerging Technologies, 86, pp.372-392.
39. Prentkovskis, O. and Junevičius, R. (2013). The research journal TRANSPORT: peer-reviewing process in 2013. *Transport*, 28(4), pp.438-442.
40. Schakel, W., Van Arem, B. and Netten, B. (2010). Effects of Cooperative Adaptive Cruise Control on traffic flow stability. 13th International IEEE Conference on Intelligent Transportation Systems. [online] Available at: https://ieeexplore.ieee.org/document/5625133 [Accessed 22 Nov. 2018].
41. Shladover, S., Desoer, C., Hedrick, J., Tomizuka, M., Walrand, J., Zhang, W., McMahon, D., Peng, H., Sheikholeslam, S. and McKeown, N. (1991). Automated vehicle control developments in the PATH program. *IEEE Transactions on Vehicular Technology*, 40(1), pp.114-130.
42. Shladover, S., Su, D. and Lu, X. (2012). Impacts of Cooperative Adaptive Cruise Control on Freeway Traffic Flow. Transportation Research Record: Journal of the Transportation Research Board, 2324(1), pp.63-70.
43. Shengbo Eben, L., Zheng, Y., Keqiang, L., Wang, L. and Hongwei, Z. (2017). Platoon Control of Connected Vehicles from a Networked Control Perspective: Literature Review, Component Modelling, and Controller Synthesis. IEEE Xplore. [online] Available at: https://ieeexplore.ieee.org/abstract/document/7970188 [Accessed 10 Oct. 2018].
44. Stevens, A., Dianati, D., Katsaros, K., Han, C., Fallah, S., Maple, C., McCullough, F. and Mouzakitis, A. (2017). Cooperative automation through the cloud. ITS European Congress 2017.
45. Su, D. and Ahn, S. (2017). In-vehicle sensor-assisted platoon formation by utilizing vehicular communications. International Journal of Distributed Sensor Networks, 13(7), p.155014771771875.
46. Sun, L., Li, Y. and Gao, J. (2016). Architecture and Application Research of Cooperative Intelligent Transport Systems. Procedia Engineering, 137, pp.747-753.
47. Surcel, M. and Shetty, M. (2015). The Impact of Design, Position and Combination of Aerodynamic Devices on Drag and Fuel Consumption. *SAE International Journal of Commercial Vehicles*, 8(2), pp.722-731.
48. Swaroop, D., Hedrick, J., Chien, C. and Ioannou, P. (1994). A Comparison of Spacing and Headway Control Laws for Automatically Controlled Vehicles1. Vehicle System Dynamics, 23(1), pp.597-625.
49. Tang, H. (2014). World Trade Report 2013 – Factors Shaping the Future of World Trade World Trade Organization,2013. *World Trade Review*, 13(04), pp.733-735.
50. Varaiya, P. (1993). Smart cars on smart roads: problems of control. *IEEE Transactions on Automatic Control*, 38(2), pp.195-207.
51. Wang, L., Syed, A., Yin, G., Pandya, A. and Zhang, H. (2014). Control of vehicle platoons for highway safety and efficient utility: Consensus with communications and vehicle dynamics. *Journal of Systems Science and Complexity*, 27(4), pp.605-631.
52. Wang, X. and Su, H. (2014). Pinning control of complex networked systems: A decade after and beyond. Annual Reviews in Control, 38(1), pp.103-111.
53. Wu, X., Qin, G., Yu, H., Gao, S., Liu, L. and Xue, Y. (2016). Using improved chaotic ant swarm to tune PID controller on cooperative adaptive cruise control. Optik, [online] 127(6), pp.3445-3450. Available at: https://www.sciencedirect.com/science/article/pii/S0030402615019233 [Accessed 18 Oct. 2018].
54. Xiao, L. and Gao, F. (2011). Practical String Stability of Platoon of Adaptive Cruise Control Vehicles. IEEE Transactions on Intelligent Transportation Systems, 12(4), pp.1184-1194.
55. Xu, L., Wang, L., Yin, G. and Zhang, H. (2015). Impact of Communication Erasure Channels on the Safety of Highway Vehicle Platoons. *IEEE Transactions on Intelligent Transportation Systems*, 16(3), pp.1456-1468.

56. Xu, L., Wang, L., Yin, G. and Zhang, H. (2014). Communication Information Structures and Contents for Enhanced Safety of Highway Vehicle Platoons. *IEEE Transactions on Vehicular Technology*, 63(9), pp.4206-4220.
57. Zhang, Y., Kosmatopoulos, B., Ioannou, P. and Chien, C. (1999). Using front and back information for tight vehicle following maneuvers. IEEE Transactions on Vehicular Technology, 48(1), pp.319-328.
58. Zheng, Y., Li, S., Li, K., Borrelli, F. and Hedrick, J. (2017). Distributed Model Predictive Control for Heterogeneous Vehicle Platoons Under Unidirectional Topologies. IEEE Transactions on Control Systems Technology, 25(3), pp.899-910.
59. Zheng, Y., Li, S., Li, K. and Ren, W. (2018). Platooning of Connected Vehicles With Undirected Topologies: Robustness Analysis and Distributed H-infinity Controller Synthesis. *IEEE Transactions on Intelligent Transportation Systems*, 19(5), pp.1353-1364.
60. Zheng, Y., Li, S., Li, K. and Wang, L. (2016). Stability Margin Improvement of Vehicular Platoon Considering Undirected Topology and Asymmetric Control. IEEE Transactions on Control Systems Technology, 24(4), pp.1253-1265.
61. Zheng, Y., Eben Li, S., Wang, J., Cao, D. and Li, K. (2016). Stability and Scalability of Homogeneous Vehicular Platoon: Study on the Influence of Information Flow Topologies. IEEE Transactions on Intelligent Transportation Systems, 17(1), pp.14-26.
62. Zhou, J. and Peng, H. (2005). Range Policy of Adaptive Cruise Control Vehicles for Improved Flow Stability and String Stability. IEEE Transactions on Intelligent Transportation Systems, 6(2), pp.229-237.

9. Appendices

Appendix 1: Relative velocity error between platoon vehicles for homogenous platoon

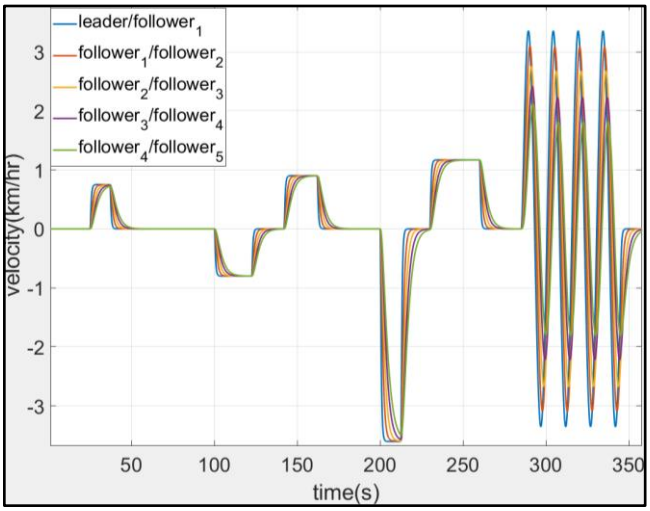

Appendix 2: Relative acceleration error between platoon vehicles for homogenous platoon

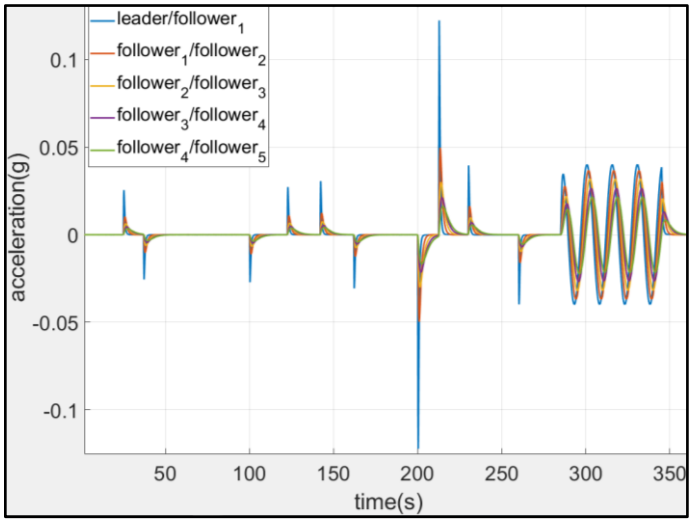

Appendix 3: Velocity profile for linear homogenous platoon

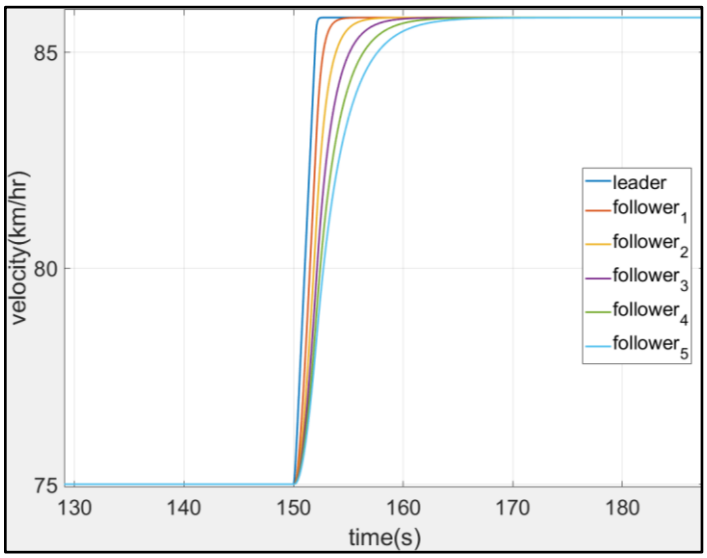

Appendix 4: Acceleration profile for linear homogenous platoon

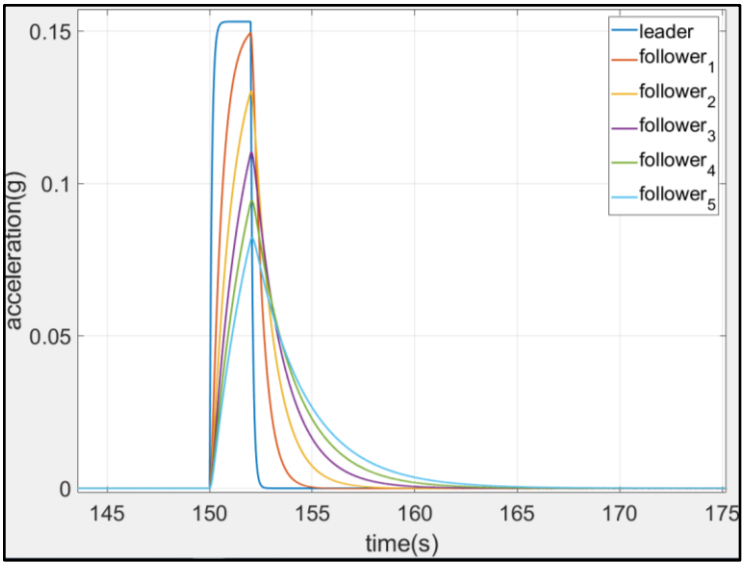

Appendix 5: Velocity profile for non-linear homogenous platoon

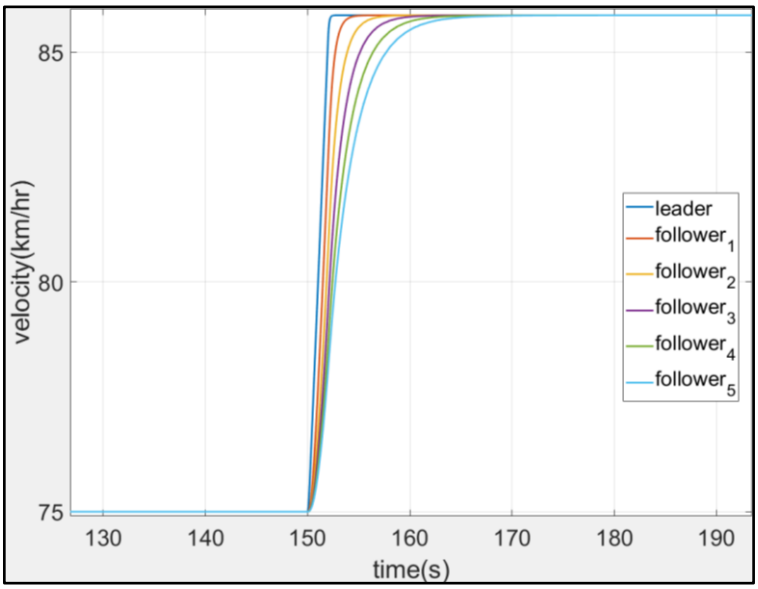

Appendix 6: Acceleration profile for non-linear homogenous platoon

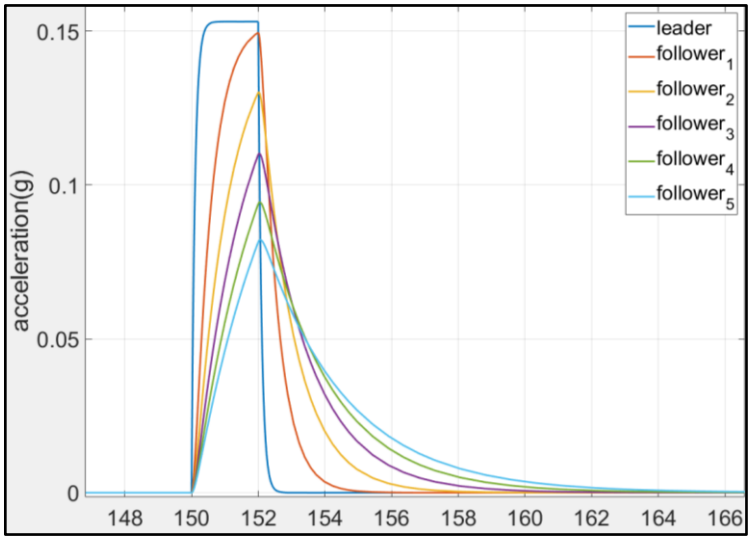

Appendix 7: PD control MATLAB variables

```
% Normal Operation & Emergency Stop Reference
Reference.v_i = [20 25 15 25 0 0];    %initial velocity
Reference.v_e = [25 15 25 0 75/3.6 70/3.6];   %final velocity
Reference.t_start = [25 100 142 200 230 285]; %initial time
Reference.t_end    =    [Reference.t_start(1)+12    Reference.t_start(2)+22.5
Reference.t_start(3)+20  Reference.t_start(4)+12.5  Reference.t_start(5)+30
Reference.t_start(6)+60];    %final time
Reference.H        =        (Reference.v_e-Reference.v_i)./(Reference.t_end-
Reference.t_start);   %height/acceleration

N = 5; % No of vehicles in the platoon
vehicleL.tau = 0.1; %[s] time constant for the leader
help_pos = 100; %Initial leader position [m]

for i=1:N

% Time gap between vehicles
controller(i).hp = 0.5; %desired time gap between preceeping vehicles (m)
controller(i).hl = 0.5; %desired time gap (m)

% PD controller parameters
controller(i).K1 = 0.038555; %gap regulating controller gains for follower
gap regulation
controller(i).K2 = 12.88408; %gap regulating controller gains for follower
vehicle gap regulation
controller(i).K3 = 1000000; %gap regulating controller gains for leader gap
regulation
controller(i).K4  =  0.005;  %gap  regulating  controller  for  leader  gap
regulation

Vehicle(i).delay =0.2; %Communications delay [s]

% Initial platoon vehicle platoon variables
%Vehicle(i).tau = 0.2*i*0.75; %Internal vehicle delay for linear driveline
dynamics
Vehicle(i).s0 = help_pos - 75/3.6*controller(i).hp; %Desired time gap between
preceeding vehicles
Vehicle(i).v0 = 75/3.6; %Initial platoon velocity (m/s)
Vehicle(i).a0 = 0;  %Initial platoon acceleration
help_pos = Vehicle(i).s0; %initial vehicle positions in the platoon
end

Err_matrix = [1 -1 0 0 0 0
0 1 -1 0 0 0
0 0 1 -1 0 0
0 0 0 1 -1 0
0 0 0 0 1 -1]; %matrix outlining mismatch between vehicles

Param.g = 9.8; % [m/s^2] acceleration due to gravity
Param.rho = 1.225; %[kg/m^3] air density

% Non-linear vehicle model
for i=1:N
Vehicle(i).A  = 2.24;          %[m^2] Front area
Vehicle(i).tau =  0.2;  %[s] internal lag [0.2-0.8] for non-linear driveline
Vehicle(i).l   =  5-i*0.1;      %[m] vehicle length []
Vehicle(i).m   =  1450;  %[kg]mass [800-1600]
Vehicle(i).eta =  0.92;  %[-] mechanical efficiency of the driveline [0.82-
0.92]
Vehicle(i).ca   =   0.38*Vehicle(i).A*Param.rho/2;     %[kg/m] coefficient of
the aerodynamic drag [0.2-0.6]
```

```
Vehicle(i).r    =  0.34;    %[m] tire radious
Vehicle(i).f    =  0.01;    %[-] coefficient of the rolling resistance

% Desired vehicle torque [Nm]
Vehicle(i).T0   =     Vehicle(i).r  ./  Vehicle(i).eta   .*   (Vehicle(i).a0.*
Vehicle(i).m   +   Vehicle(i).ca   .*   Vehicle(i).v0.^2   +   Vehicle(i).m   .*
Vehicle(i).f .* Param.g); % Desired vehicle torque[Nm]

end
vel_pos = [1 0 0]; %position state [m]
vel_vet = [0 1 0]; %velocity state [km/hr]
vel_acc = [0 0 1]; %acceleration state [g]
```

Appendix 8: Non-linear Simulink vehicle model

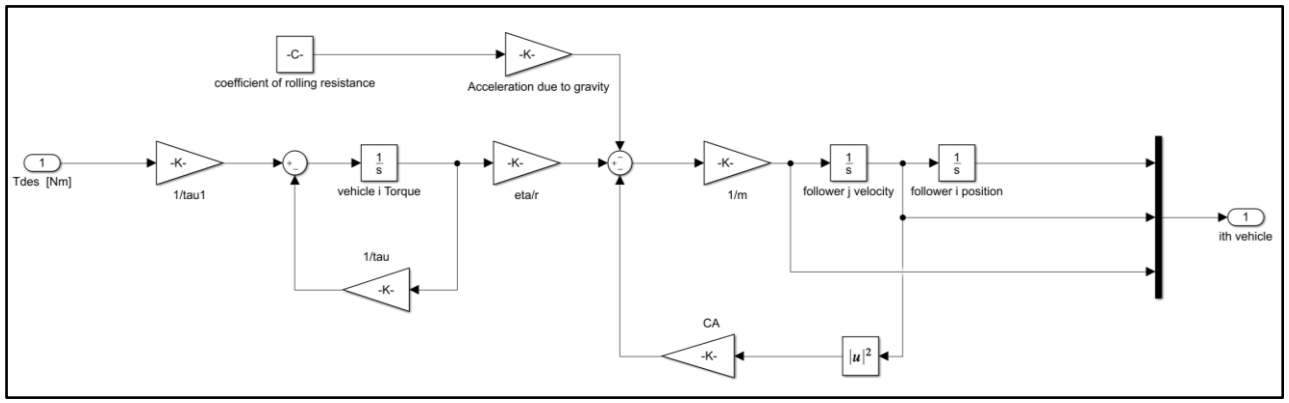

Appendix 9: PD controller Simulink block model

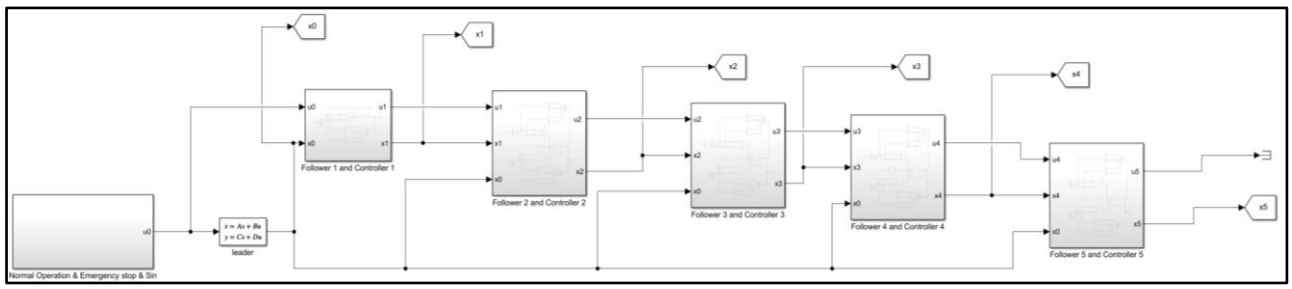

Appendix 10: PD structure controller model